TRAVELLING WAVE SOLUTIONS

A dissertation submitted to the University of Manchester
for the degree of Master of Science
in the Faculty of Science and Engineering

2016

Rami Achouri
School of Mathematics

Contents

List of Tables

List of Figures

Abstract

In this project, the dynamics of the Burgers-Huxley equation and the FitzHugh-Nagumo equations are explored. A set of numerical methods are implemented in favour of approximately solving the non-linear equations. We determined an infinite number of solutions for the Burgers-Huxley equation with the use of phase plane analysis and power series approximations. The FitzHugh-Nagumo equations are shown to omit a set of distinct solutions with regards to a variation of its parameters. A strong relation has been established between the magnitude of the pulse wave and with its speed. We then implement a singular perturbation method to explore the concept behind the construction of an approximate analytical solution for the FitzHugh-Nagumo equations. Finally, an explicit solution for the speed of the pulse wave is determined, to which we then validate numerically.

Declaration

No portion of the work referred to in the dissertation has been submitted in support of an application for another degree or qualification of this or any other university or other institute of learning.

Intellectual Property Statement

The University Library's regulations (see http://www.manchester.ac.uk/library/aboutus/regulations) and in The University's Guidance on Presentation of Dissertations.

Acknowledgements

I would like to thank Dr Yanghong Huang for his time, support and for being a very good supervisor. I would like to dedicate this project to my parents.

Chapter 1

Introduction

The use of partial differential equations (PDEs) in today's world is ubiquitous in many fields of study. The importance of studying and applying such equations stems from a dynamical perspective of the complexities of physical models. Euler, Lagrange and d'Alembert were one of the first people to make use of PDEs in describing the mechanics of continua and as a basis for studying models analytically in physical science [6]. As such, the focal aim of this project is to study a particular class of PDEs that exhibit travelling wave solutions. The PDEs are known as the *Burgers-Huxley* and *FitzHugh-Nagumo* equations that are non-linear in nature. Furthermore, the aim of this project extends to determining the existence of solutions for the stated equations. The motivation towards analysing such equations arises from the methodological treatment conducted by others in favour of exploring for their dynamics and applications. Within this project, a couple of powerful methods will be considered to solve the aforementioned equations explicitly and numerically.

The material in this project is structured as follows. In Chapter 2, the background material on travelling wave solutions is introduced. The chapter then leads onto the exploration of different methods that may be applied to solve the aforementioned equations. In Chapter 3, The dynamics of the Burgers-Huxley equation is investigated, with respect to the parameters associated with the equation. This is done via the use of a numerical scheme. A phase plane analysis is then conducted in favour of investigating the system further. In Chapter 4, The FitzHugh-Nagumo equations

are introduced. The dynamics of the equations are explored with regards to the parameters of the system. The chapter then concludes with the implementation of a singular perturbation method. Finally, chapter 5 corresponds to the conclusion, where the area of further research is explored.

Chapter 2

Background Material

In this chapter, the theory behind travelling waves is introduced, where two PDEs are solved analytically, in favour of illustrating the different forms of travelling waves that exist. The difficulty behind solving non-linear PDEs is addressed, resulting in the exploration of many powerful methods for solving non-linear PDEs numerically and analytically. The chapter then concludes with a detailed description on the factorisation and finite difference methods, which were selected for solving the FitzHugh-Nagumo and Burgers-Huxley equations, where appropriate.

2.0.1 Travelling Waves

A *travelling wave* is a wave that advances in a particular direction, with the addition of retaining a fixed shape. Moreover, a travelling wave is associated to having a constant velocity throughout its course of propagation. Such waves are observed in many areas of science, like in combustion, which may occur as a result of a chemical reaction [26]. In mathematical biology, the impulses that are apparent in nerve fibres are represented as travelling waves [21]. Also, in conservations laws associated to problems in fluid dynamics, shock profiles are characterised as travelling waves [24]. Furthermore, the structures present in solid mechanics are typically modelled as standing waves [8]. Hence, it is important to determine the dynamics of such solutions. On a similar note, the importance towards analysing the Burgers-Huxley and FitzHugh-Nagumo equations within this project stems from a similar basis. A travelling wave solution

is obtained upon solving a model that corresponds to a system. Generally, these models take the forms of partial differential equations (PDEs), where the dynamics of the systems are comprehended upon solving for solutions. These travelling wave solutions are expressed as $u(x,t) = U(z)$, where $z = x - ct$. Here, the spatial and time domains are represented as x and t, with the velocity of the wave given as c. If $c = 0$, the resulting wave is named a *stationary wave*. Such waves do not propagate, and are typically observed when inducing a fixed boundary. In fact, we can categorise travelling waves into forms that are attributed to having certain properties (Figure 2.1). For a travelling wave that approaches constant states given by $U(-\infty) = u_l$ and $U(\infty) = u_r$, with $u_l \neq u_r$, we have what we call a *wave front*. However, if the constant states are equal with $u_l = u_r$, the corresponding wave is known as a *pulse wave*. If a wave exhibits periodicity with $U(z + F) = U(z)$, where $F > 0$, the wave is called a *spatially periodic wave*.

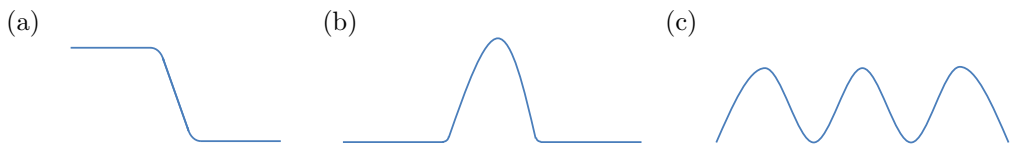

Figure 2.1: Forms of travelling waves: (a) wave front, (b) pulse and (c) spatially periodic travelling wave.

To elaborate further on the different forms of travelling waves, we shall derive geometrical representations of such solutions. Consider the following *Burgers* equation, associated with advection and dispersion:

$$u_t = \alpha u_{xx} - u u_x. \tag{2.1}$$

We start by setting $u(x,t) = U(z) = U(x - ct)$, with boundary conditions of $U(-\infty) = u_l$ and $U(\infty) = u_r$. Upon replacing the partial derivatives of u in equation (2.1), with the appropriate derivatives in U, we get

$$-cU' = \alpha U'' - UU'.$$

From here, we can integrate to obtain

$$-cU = \alpha U' - \frac{U^2}{2} + d, \tag{2.2}$$

where d is a constant of integration. We can now make use of the boundary condition $U(\infty) = u_r$ with $U'(\infty) = 0$, to get

$$d = \frac{u_r^2}{2} - cu_r.$$

Thus, we can obtain an explicit expression for the wave speed c, after applying the boundary condition of $U(-\infty) = u_l$, with $U'(-\infty) = 0$. This leads to

$$-cu_l = \frac{-u_l^2}{2} + \frac{u_r^2}{2} - cu_r, \tag{2.3}$$

after which we solve for c, to get

$$c = \frac{u_r + u_l}{2}. \tag{2.4}$$

Upon observation, it is apparent that the speed of the wave is directly dependent on the far field boundary values. Continuing with our derivation, equation (2.2) becomes,

$$-cU = \alpha U' - \frac{U^2}{2} + \frac{u_r^2}{2} - cu_r. \tag{2.5}$$

We now rearrange (2.5), in favour of isolating the $\alpha U'$ term, yielding

$$\alpha U' = \frac{U^2}{2} - cU - \frac{u_r^2}{2} + cu_r.$$

This equation is separable, and can be re-expressed into a form that will enable us to integrate it directly. The equivalent form is given by,

$$\frac{2\alpha dU}{U^2 - 2cU - u_r^2 + 2cu_r} = dz. \tag{2.6}$$

We can determine the existence of solutions by considering the two cases of having $u_l > u_r$ and $u_l < u_r$. To do this, we substitute (2.4) into (2.6), and rearrange the resulting expression for $\frac{dU}{dz}$, to get

$$\frac{dU}{dz} = \frac{U^2 - (u_r + u_l)U + u_l u_r}{2\alpha}. \tag{2.7}$$

The expression in on the right hand side can be factored, giving

$$\frac{dU}{dz} = \frac{(U - u_r)(U - u_l)}{2\alpha}. \tag{2.8}$$

If $0 < u_l < u_r$, then $\frac{dU}{dz} < 0$, since $u_l < U < u_r$. However, the solution U will not be contained within the defined boundary, and thus a solution cannot exist. On the other hand, if $0 < u_r < u_l$, we have $u_r < U < u_l$ and $\frac{dU}{dz} < 0$. Hence a solution exists. The simplistic approach taken to determine the existence of solutions cannot be adapted for the FitzHugh-Nagumo or the Burger-Huxley equations. Since the equations are non-linear, they will require the implementation of a more complicated process to prove the existence of solutions, if applicable.

Further to our derivation, we can integrate equation (2.6), resulting in

$$2\alpha \int_g^U \frac{dm}{m^2 - 2cm - u_r^2 + 2cu_r} = z. \tag{2.9}$$

where $U(0) = g$. Upon setting $u_l = 1$ and $u_r = 0$, we can obtain a particular solution. Thus from (2.4), we get $c = \frac{1}{2}$. Furthermore, by setting $g = \frac{1}{2}$, equation (2.9) becomes

$$2\alpha \int_{\frac{1}{2}}^U \frac{dm}{m^2 - m} = z. \tag{2.10}$$

We can now integrate equation (2.10), after which we then solve for $U(z)$ to obtain,

$$U(z) = \frac{1}{1 + e^{\frac{z}{2\alpha}}}. \tag{2.11}$$

Finally, the travelling wave solution in $u(x,t)$ is given by,

$$u(x,t) = \frac{1}{1 + e^{\frac{x-ct}{2\alpha}}} \tag{2.12}$$

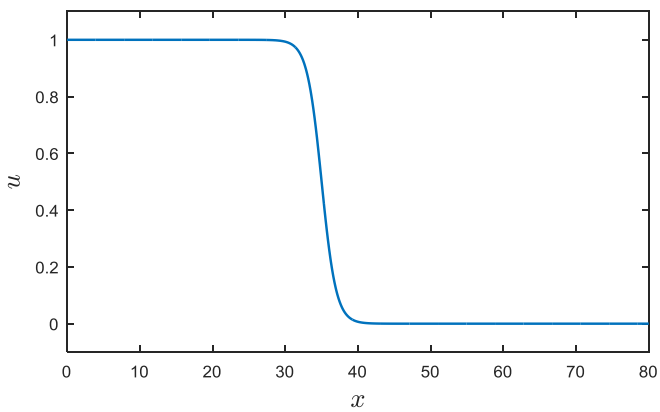

Figure 2.2: Travelling wave front solution with $u_l = 1, u_r = 0$, $c = \frac{1}{2}$ and $\alpha = 0.5$.

The travelling wave solution present in Figure 2.2 corresponds to a wave front, which propagates towards the right of the spacial domain with respect to increasing time. Wave fronts are observed in chemical kinetics such as in frontal polymerization and in cold flames [22].

We can emulate a similar approach to solve for a solution that takes the form of a pulse wave. The equation of interest is known as the *Korteweg-de Vries* (KdV) equation, and is defined as

$$u_t + 6uu_x + u_{xxx} = 0. \tag{2.13}$$

The KdV equation is applied to model waves that are located on shallow water surfaces [12]. The non-linear equation is associated to having travelling wave solutions, defined as

$$u(x,t) = U(z) = U(x - ct). \tag{2.14}$$

Hence, the solution u implies that U is a solution to

$$-cU' + 6UU' + U''' = 0, \tag{2.15}$$

where $' = \frac{d}{dz}$. We can integrate (2.15) to get,

$$-cU + 3U^2 + U'' = n, \tag{2.16}$$

where n is a constant of integration. Upon multiplying (2.16) with U', we obtain

$$-cUU' + 3U^2U' + U''U' = nU'. \tag{2.17}$$

We now integrate equation (2.17), giving

$$\frac{(U')^2}{2} = -U^3 + \frac{c}{2}U^2 + nU + m, \tag{2.18}$$

where m is a constant of integration. Since it is desired that we obtain a pulse wave solution, we require $U, U', U'' \to 0$ as $z \to \pm\infty$. As a consequence, the constants $n = m = 0$. Thus, equation (2.18) simplifies to

$$\frac{(U')^2}{2} = \frac{cU^2}{2} - U^3. \tag{2.19}$$

From here, we can solve for U', to obtain

$$U' = \pm U(c - 2U)^{\frac{1}{2}}. \tag{2.20}$$

To simplify calculations, we shall choose the negative sign in (2.20). This ordinary differential equation (ODE) can be integrated directly from an alternate form, given by

$$\frac{-dU}{U(c-2U)^{\frac{1}{2}}} = dz. \tag{2.21}$$

Thus, we integrate to get

$$z = -\int_{\frac{c}{2}}^{U(z)} \frac{dw}{w(c-2w)^{\frac{1}{2}}} + d, \tag{2.22}$$

where d is an arbitrary constant. We now introduce a substitution of $w = \frac{c}{2}\operatorname{sech}^2\theta$, to aid in the integration process of the right hand side of equation (2.22). As a result, we have $\dfrac{dw}{d\theta} = -c\operatorname{sech}^2\theta\tanh\theta$. The denominator of the integrand in (2.22) becomes,

$$\begin{aligned} w(c-2w)^{\frac{1}{2}} &= \frac{c}{2}\operatorname{sech}^2\theta\left[c - 2\left(\frac{c}{2}\operatorname{sech}^2\theta\right)\right]^{1/2} \\ &= \frac{c}{2}\operatorname{sech}^2\theta\sqrt{c\left(1-\operatorname{sech}^2\theta\right)} \\ &= \frac{c^{\frac{3}{2}}}{2}\operatorname{sech}^2\theta\tanh\theta. \end{aligned}$$

After introducing the stated substitution for w, we can integrate (2.22) explicitly, giving

$$z = \frac{2}{\sqrt{c}}\theta + d, \tag{2.23}$$

where θ is defined implicitly as

$$\frac{c}{2}\operatorname{sech}^2\theta = U(z). \tag{2.24}$$

Upon rearranging (2.23) in terms of θ, we obtain

$$\theta = \frac{\sqrt{c}}{2}(z-d). \tag{2.25}$$

We now substitute (2.25) into (2.24), to get

$$U(z) = \frac{c}{2}\operatorname{sech}^2\left(\frac{\sqrt{c}}{2}(z-d)\right).$$

Hence, the travelling wave solution is given by,

$$u(x,t) = \frac{c}{2}\operatorname{sech}^2\left(\frac{\sqrt{c}}{2}(x-ct-d)\right).$$

with $x \in \mathbb{R}, t \geq 0$. As of this result, we can observe that there is a relation between the amplitude of the wave and its speed.

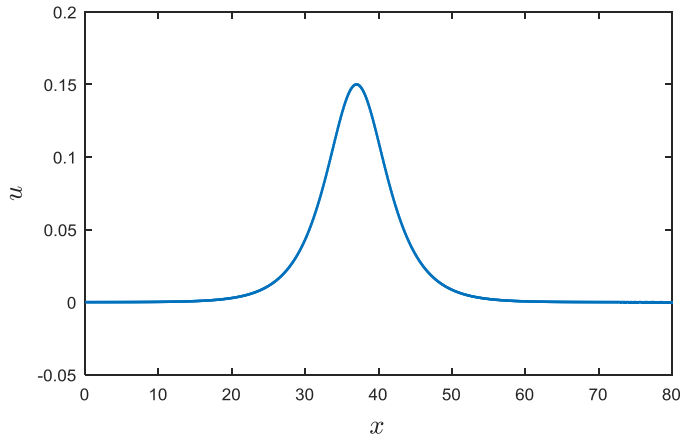

Figure 2.3: Pulse wave solution with $u_l = u_r = 0$ and $c = 0.3$.

The pulse wave solution of the KdV equation is present in Figure 2.3. Such a solution has been obtained via a method that cannot be generalised to solving more difficult PDEs. On a general basis, the methods employed to obtaining solutions of different classes of PDEs require more complex and vigorous approaches. There are many non-linear PDEs that remain to be solved analytically. Unfortunately, the FitzHugh-Nagumo equations fall into this category, where an analytical solution is sought-after. On the contrary, the Burgers-Huxley equation may be solved analytically in favour of obtaining special solutions. We shall explore some of the possible methods to solving non-linear PDEs analytically and numerically in the following section.

2.0.2 Methods for Solving Non-linear PDEs

Most non-linear PDEs require powerful and robust methods to solve for an explicit solution. Fan [13] used the tanh-function method to obtain explicit solutions to non-linear PDEs. The method was adopted later to solve for exact travelling wave solutions of the generalised Hirota Satsuma coupled KdV system, the double Sine-Gordon equation and the Schrdinger equation [11]. The first-integral method, related to the ring theory of commutative algebra, was used by Hossein et al [18], to obtain a class of travelling wave solutions for the Davey-Stewartson equation. Another method of interest is known as the factorisation method, which was employed by Cornejo-Pérez and Rosu [9] to solve the generalised Liénard equation. The method was praised for

its simplistic and efficient ways for solving non-linear PDEs. The Homotopy analysis method (HAM) has been used extensively for solving many non-linear problems in science and engineering [29]. Rashidi et al [23] applied this method to obtain the soliton solution of the coupled Whitham-Broer-Kaup equations in shallow water. They claimed that the HAM is one of the most effective methods to solving non-linear problems, and introduces new ways to obtaining series solutions of these problems. The Exp-function method was proposed by He and Wu [16], to seeking solitary and periodic solutions of non-linear differential equations. Their equations of choice were the KdV and Dodd-Bullough-Mikhailov equations. The method was illustrated to being a convenient and effective method, and was stated to being one of the most versatile tools applicable to non-linear engineering problems. There are many other methods that could be considered, namely, the sine-cosine method, the F-expansion method, the Jacobi elliptic function expansion method, etc.

Many PDEs do not have exact solutions, and thus require the use of numerical methods to solve for approximate solutions. There are many numerical methods to approximately solve non-linear PDEs. Kamal implemented the Sinc collocation method to solve Fisher's reaction-diffusion equation [10]. He also used the Sinc-Galerkin method to approximate the solution for the Korteweg-de Vries model equation [4]. The finite difference method was applied by Wensheng and Yunyin [28] to obtain approximate solutions of boundary value problems for a specific form of the Helmholtz equation. Hariharan et al [15] adopted the Haar wavelet method to solve Fisher's equation. They demonstrated that the accuracy of the solution was high even for a smaller number of grid points. There are other numerical methods that could be used. To name a few, the polynomial differential method, the cubic B-spline method, the Runge-Kutta method and so on.

In this project, we will employ the factorisation method to solve the Burgers-Huxley equation analytically, and the finite difference method to solve this equation, and the FitzHugh-Nagumo equations numerically, with the use of MATLAB. The theory behind the analytical and numerical methods of choice will be explored in the following subsequent sections.

Factorisation Method

The method that will be employed to solve the Burgers-Huxley equation is known as the factorisation method. It is a method that seeks travelling wave solutions for a particular class of PDEs that are associated with having a polynomial non-linearity. In order to illustrate the procedure involved, we will implement the method to a non-linear PDE from a general perspective. Consider a PDE of the form

$$u_{tt} - u_x = h(u), \tag{2.26}$$

where the $h(u)$ term corresponds to the polynomial non-linearity of the equation. We introduce a travelling wave ansatz of the form $u(x,t) = U(z)$, where $z = p(x-ct)$. The constants p and c represent the wave number and the velocity of the wave respectively. We now rescale the equation in favour of eliminating the coefficient of the highest order derivative. As a consequence, the resulting ODE becomes

$$\frac{d^2U}{dz^2} + G(U)\frac{dU}{dz} + F(U) = 0, \tag{2.27}$$

where $G(U) = \frac{c}{p}$ and $F(U) = \frac{1}{p^2}h(u)$. The aim involved is to factorise equation (2.27) into a form given by

$$[D - f_2(U)][D - f_1(U)]\, U = 0, \tag{2.28}$$

where $D = \frac{d}{dz}$ and where functions f_1 and f_2 relate to $F(U)$ implicitly. From here, we will take a reverse chronological approach to establish the relation between (2.27) and (2.28). To do this, we start by expanding (2.28) to get

$$D^2U - Df_1U - f_2DU + f_1f_2U = 0. \tag{2.29}$$

With the use of the chain rule, equation (2.29) leads to

$$\frac{d^2U}{dz^2} - f_1\frac{dU}{dz} - \frac{df_1}{dU}\frac{dU}{dz}U - f_2\frac{dU}{dz} + f_1f_2U = 0. \tag{2.30}$$

At this point, it is required that we factorise the expression in (2.30) by gouping terms. There are two possible ways to do this. Berkovich [5] propossed the following grouping method:

$$\frac{d^2U}{dz^2} - (f_2 + f_1)\frac{dU}{dz} + \left(f_2f_1 - \frac{df_1}{dU}\frac{dU}{dz}\right) U = 0. \tag{2.31}$$

At a later stage, Cornejo-Pérez and Rosu [9] introduced a grouping technique that was stated to being more favourable for its uses. As such, we will be using this method of grouping which is given by,

$$\frac{d^2U}{dz^2} - \left(\frac{df_1}{dU}U + f_2 + f_1\right)\frac{dU}{dz} + f_1 f_2 U = 0. \tag{2.32}$$

By comparison between (2.32) and (2.27), we get

$$\frac{df_1}{dU}U + f_2 + f_1 = -G(U), \tag{2.33}$$

and

$$f_1 f_2 = \frac{F(U)}{U}. \tag{2.34}$$

From equation (2.33), we can obtain relations and expressions for some of the unknown terms. Moreover, It can be established that the ODE present in (2.28) defined as $[D - f_1]\,U = 0$ is compatible with equation (2.27). Finally, the solutions to this first order ODE will lead to solutions to the general equation considered in (2.26).

Finite Difference Method

The finite difference method is associated with the replacement of derivatives in a PDE, with *finite difference approximations*. This leads to the formation of *finite difference schemes*, which consist of large algebraic systems of equations that may be solved, in favour of obtaining approximate solutions. To derive finite difference approximations to partial derivatives, we initialise by setting the solution u to be a function of the independent variables x and t only. This choice of variables is based on the PDEs considered in this thesis. Holding t fixed, we can make use of Taylor's formula to expand u about a point x_0, obtaining

$$u(t, x_0 + \Delta x) = u(t, x_0) + \Delta x\, u_x(t, x_0) + \ldots + \frac{(\Delta x)^{n-1}}{(n-1)!}u_{n-1}(t, x_0) + O(\Delta x^n), \tag{2.35}$$

where Δx is the spacing between points in the discretized domain. This representation of u can be manipulated to obtain different orders of finite difference expressions. For a simplistic case, we truncate (2.35) to order Δx^2 giving,

$$u(t, x_0 + \Delta x) = u(t, x_0) + \Delta x\, u_x(t, x_0) + O(\Delta x^2). \tag{2.36}$$

The partial derivative u_x can be rearranged for to get,

$$u_x(t, x_0) = \frac{u(t, x_0 + \Delta x) - u(t, x_0)}{\Delta x} - O(\Delta x). \tag{2.37}$$

The representation of u_x in (2.37) holds true for any point x_i in a continuous domain, at an instance in time t_j. Also, to avoid clutter of notation, let $u(t_j, x_i) = u_i^j$. Hence, introducing the general notation of t_j and x_i, (2.37) can be expressed as,

$$u_x(t_j, x_i) = \frac{u_{i+1}^j - u_i^j}{\Delta x} - O(\Delta x). \tag{2.38}$$

Neglecting the $O(\Delta x)$ term in (2.38), we get

$$u_x(t_j, x_i) \approx \frac{u_{i+1}^j - u_i^j}{\Delta x}, \tag{2.39}$$

which is known as the *forward difference* approximation. It is a first order approximation, illustrated by the $O(\Delta x)$ term that we discarded.

On a related note, we can derive the *backwards difference* approximation in a similar manner. Taking the expression for u in (2.36) and substituting Δx for $-\Delta x$ gives,

$$u(t, x_0 - \Delta x) = u(t, x_0) - \Delta x\, u_x(t, x_0) + O(\Delta x^2). \tag{2.40}$$

To generalise, we rearrange (2.40) in terms of u_x and we introduce t_j and x_i as done previously to get,

$$u_x(t_j, x_i) \approx \frac{u_i^j - u_{i-1}^j}{\Delta x}, \tag{2.41}$$

where the $O(\Delta x)$ term has been dropped. It should be noted that we can derive more accurate finite difference approximations by including higher order terms when truncating the expression for u in (2.35) during the derivation process.

We shall now derive a finite difference approximation for a second order partial derivative u_{xx}. We start by truncating the expansion present in (2.35) up to order Δx^4.

$$u(t, x_0 + \Delta x) = u(t, x_0) + \Delta x\, u_x(t, x_0) + \frac{(\Delta x)^2}{2} u_{xx}(t, x_0) + \frac{(\Delta x)^3}{6} u_{xxx}(t, x_0) + O(\Delta x^4). \tag{2.42}$$

From here, we can substitute $-\Delta x$ into (2.42) to replace Δx giving,

$$u(t, x_0 - \Delta x) = u(t, x_0) - \Delta x\, u_x(t, x_0) + \frac{(\Delta x)^2}{2} u_{xx}(t, x_0) - \frac{(\Delta x)^3}{6} u_{xxx}(t, x_0) + O(\Delta x^4). \tag{2.43}$$

Combining (2.42) and (2.43) by addition gives,

$$u(t, x_0 + \Delta x) + u(t, x_0 - \Delta x) = 2u(t, x_0) + (\Delta x)^2 u_{xx}(t, x_0) + O(\Delta x^4). \tag{2.44}$$

Introducing the general notation with $u_i^j = u(t_j, x_i)$ and then rearranging for u_{xx}, we get

$$u_{xx}(t_j, x_i) = \frac{u_{i+1}^j - 2u_i^j + u_{i-1}^j}{\Delta x^2} - O(\Delta x^2). \tag{2.45}$$

Dropping the $O(\Delta x^2)$ error term in (2.45) gives the *symmetric difference* approximation which is of second order. The methods involved in deriving such equations can be replicated for the independent variable t holding x fixed, yielding the same results. For further insight, a list of finite difference approximations are present in Table 2.1 with their respective orders.

Table 2.1: Finite Difference Approximations.

Partial derivative	FD approximation	Classification	Order
u_x	$\dfrac{u_i^j - u_{i-1}^j}{\Delta x}$	backward	$O(\Delta x)$
u_x	$\dfrac{u_{i+1}^j - u_i^j}{\Delta x}$	forward	$O(\Delta x)$
u_x	$\dfrac{u_{i+1}^j - u_{i-1}^j}{2\Delta x}$	central	$O(\Delta x^2)$
u_{xx}	$\dfrac{u_{i+1}^j - 2u_i^j + u_{i-1}^j}{(\Delta x)^2}$	symmetric	$O(\Delta x^2)$
u_t	$\dfrac{u_i^j - u_i^{j-1}}{\Delta t}$	backward	$O(\Delta t)$
u_t	$\dfrac{u_i^{j+1} - u_i^j}{\Delta t}$	forward	$O(\Delta t)$
u_t	$\dfrac{u_i^{j+1} - u_i^{j-1}}{2\Delta t}$	central	$O(\Delta t^2)$
u_{tt}	$\dfrac{u_i^{j+1} - 2u_i^j + u_i^{j-1}}{(\Delta t)^2}$	symmetric	$O(\Delta t^2)$

Many finite difference schemes can be constructed with the use of the finite difference approximations present in Table 2.1. The choice of a scheme to be implemented for a particular problem extends to its advantages and disadvantages, as some schemes are efficient in producing approximate solutions at a faster rate than others that are

more efficient in producing accurate results. Furthermore, most schemes consist of limitations to which they may approximate a solution. Such limitations, if violated, will results in infeasible approximate solutions. We have now introduced all the underlying theory behind the methods of choice. Therefore, we shall start by analysing the Burgers-Huxley equation in the following chapter.

Chapter 3

Burgers-Huxley Equation

Within this chapter, the Burgers-Huxley equation is introduced, and an explicit finite difference scheme is constructed, in favour of solving the equation numerically. The accuracy and the order of the scheme is then defined. After this segment, the phenomenon of a shifting wave is addressed, where a shifting technique is implemented, to simulate a travelling wave solution. Numerical solutions associated to a variation in parameters are then presented. The Burgers-Huxley equation is then solved analytically with the use of the factorisation method, where a set of special solutions are obtained. The chapter then leads onto an investigation of the qualitative behaviour of the dynamical system associated with the Burgers-Huxley equation. This has been done with the use of phase plane analysis techniques. In the final section of this chapter, the existence of solutions is explored, with the use of power series approximations, in favour of obtaining feasible travelling wave solutions.

The Burgers-Huxley equation is defined as,

$$u_t + u^k u_x = u_{xx} + u^m(1 - u^n). \tag{3.1}$$

where the parameter k, m and n are positive integers. The Burgers-Huxley equation is widely used to model the dynamics of a range of physical phenomenon that may be attributed to having reaction mechanisms. For example, the equation is used to describe the dynamics of electric pulses that occur in nerve fibres and wall in liquid crystals [27]. Furthermore, the equation is used to model the interactions between diffusion transports and convection/advection effects [3]. Within the next section,

we shall start by deriving a numerical scheme, to solve the aforementioned equation numerically.

3.1 Explicit Finite Difference Scheme

For the Burgers-Huxley equation, we will derive an *explicit scheme*. As the name may suggest, an explicit scheme is referred to as a *time-marching scheme* where the solutions to a function u at a time level $j+1$ are approximated with the use of solutions at the previous time level, j. This dependence is what classifies the scheme as being explicit, since the solutions at a previous instance in time are known, resulting in an expression that does not require solving. On the contrary, when it is required that we solve a system of equations to obtain solutions at a later instance in time, we have what we call an *Implicit scheme*. Further to our derivation of the explicit scheme, consider the the Burgers-Huxley equation in (3.1), defined as

$$u_t + u^k u_x = u_{xx} + u^m(1 - u^n). \tag{3.2}$$

It is required that we approximate the partial derivatives in u with the use of finite difference approximations. In order to adhere to the requirements of an explicit scheme, we select the following approximations from Table 2.1:

$$u_t = \frac{u_i^{j+1} - u_i^j}{\Delta t},\ u_x = \frac{u_{i+1}^j - u_{i-1}^j}{2\Delta x},\ u_{xx} = \frac{u_{i+1}^j - 2u_i^j + u_{i-1}^j}{(\Delta x)^2}. \tag{3.3}$$

Upon substituting the approximations at (3.3) into the equation, we get

$$\frac{u_i^{j+1} - u_i^j}{\Delta t} = \frac{u_{i+1}^j - 2u_i^j + u_{i-1}^j}{(\Delta x)^2} - \left(u_i^j\right)^k \left(\frac{u_{i+1}^j - u_{i-1}^j}{2\Delta x}\right) + \left(u_i^j\right)^m \left(1 - \left(u_i^j\right)^n\right). \tag{3.4}$$

We now rearrange for u_i^{j+1}, giving

$$u_i^{j+1} = u_i^j + \frac{\Delta t}{(\Delta x)^2}\left(u_{i+1}^j - 2u_i^j + u_{i-1}^j\right) - \frac{\Delta t}{2\Delta x}\left(u_i^j\right)^k \left(u_{i+1}^j - u_{i-1}^j\right) + \Delta t\ \left(u_i^j\right)^m \left(1 - \left(u_i^j\right)^n\right), \tag{3.5}$$

which concludes the derivation of the explicit scheme. Here we can see that the unknown and known terms have been moved to the left and right hand sides of the equation respectively. Thus, upon iteration, we can obtain approximate solutions to the unknown terms defined at the next successive time step. The accuracy of such

solutions would depend primarily on the accuracy of the scheme. Hence, it is important to explorer the error associated with a scheme, in favour of obtaining approximate solutions to a required accuracy. As such, we will determine the error involved for the explicit scheme (3.5) in the following section.

3.1.1 Accuracy of Scheme

A finite difference scheme is said to be *consistent* with a PDE if the error involved diminishes as the step size in time and space tends to zero. This condition is mandatory for the convergence of solutions to be achieved. The order of accuracy of a scheme directly relates to the truncation error associated with the reduction of the finite difference approximations. The accuracy of a scheme can be determine in a couple of ways. The approach that we will be taking consists of Taylor expanding terms within the scheme about (t_j, x_i), extracting the original equation with additional error terms that will correspond to the accuracy of the scheme. To do this, we start by taking the rearranged form of the explicit scheme given by

$$\frac{u_i^{j+1} - u_i^j}{\Delta t} - \frac{u_{i+1}^j - 2u_i^j + u_{i-1}^j}{(\Delta x)^2} + \left(u_i^j\right)^k \left(\frac{u_{i+1}^j - u_{i-1}^j}{2\Delta x}\right) - \left(u_i^j\right)^m \left(1 - \left(u_i^j\right)^n\right) = 0. \quad (3.6)$$

To simplify calculations, we will examine equation (3.6) on a term by term basis. Thus, the first term becomes

$$\frac{u_i^{j+1} - u_i^j}{\Delta t} = \frac{u_i^j + \Delta t\, u_t + O(\Delta t^2) - u_i^j}{\Delta t} = u_t + O(\Delta t). \quad (3.7)$$

Similarly, we can express the second term as

$$\begin{aligned}\frac{u_{i+1}^j - 2u_i^j + u_{i-1}^j}{(\Delta x)^2} =& \frac{\left[u_i^j + \Delta x\, u_x + \frac{(\Delta x)^2}{2} u_{xx} + \frac{(\Delta x)^3}{6} + O(\Delta x^4)\right] - 2u_i^j}{(\Delta x)^2} \\ &+ \frac{\left[u_i^j - \Delta x\, u_x + \frac{(\Delta x)^2}{2} u_{xx} - \frac{(\Delta x)^3}{6} + O(\Delta x^4)\right]}{(\Delta x)^2} = u_{xx} + O(\Delta x^2).\end{aligned} \quad (3.8)$$

Likewise, the third term becomes

$$\begin{aligned}\left(u_i^j\right)^k\left(\frac{u_{i+1}^j-u_{i-1}^j}{2\Delta x}\right) =& \frac{\left(u_i^j\right)^k\left[u_i^j+\Delta x\, u_x+\frac{(\Delta x)^2}{2}u_{xx}+O(\Delta x^3)\right]}{2\Delta x} \\ &- \frac{\left(u_i^j\right)^k\left[u_i^j-\Delta x\, u_x+\frac{(\Delta x)^2}{2}u_{xx}+O(\Delta x^3)\right]}{2\Delta x} \\ &= \left(u_i^j\right)^k u_x+O(\Delta x^2).\end{aligned} \tag{3.9}$$

Substituting (3.7), (3.8) and (3.9) into equation (3.6) gives

$$u_t+O(\Delta t)-u_{xx}-O(\Delta x^2)+\left(u_j^i\right)^k u_x+O(\Delta x^2)-\left(u_i^j\right)^m\left(1-\left(u_i^j\right)^n\right)=0.$$

Finally, we drop the index notation and rearrange to get

$$u_t+u^k u_x=u_{xx}+u^m\left(1-u^n\right)+O(\Delta t)+O(\Delta x^2). \tag{3.10}$$

Looking at (3.10), we can see that the additional error terms are first order in time and second order in space. Thus, the error involved will diminish and tend to zero as $\Delta t, \Delta x \to 0$. As a result, we can conclude that the explicit scheme is consistent with the Burgers-Huxley equation. Moreover, it would fit our particular agenda to minimize Δx and to maximize Δt, in favour of obtaining accurate solutions within a shortest amount of time possible. However, consistency does not signify that a scheme will converge to a solution for any predefined Δt and Δx. Thus a choice for Δx and Δt, will be obtained upon numerical experiments. In the following section, we shall explore the method behind simulating a travelling wave solution.

3.2 Numerical Results

3.2.1 Shifting of a Travelling Wave

A travelling wave will propagate at a constant velocity in a particular direction. If we were to superimpose a boundary along its course in finite space, the wave will reach the boundary over a set period of time. The solution thereof will not be representative of a travelling wave. The finite difference method requires that we solve the PDE over a fixed domain, invoking this additional problem. To overcome this restriction,

a shifting technique has been implemented that allows a travelling wave to propagate freely over an unrestricted domain. To illustrate the technique involved, we initialize by introducing superficial Dirichlet boundary conditions of $u(-L) = 1$ and $u(L) = 0$ with $L \in \mathbb{R}$, in favour of replacing the far field conditions of $u(-\infty) = 1$ and $u(\infty) = 0$. Upon discretising the domain, the time-marching scheme is executed and we obtain an approximated wave solution of the form given in Figure 3.1.

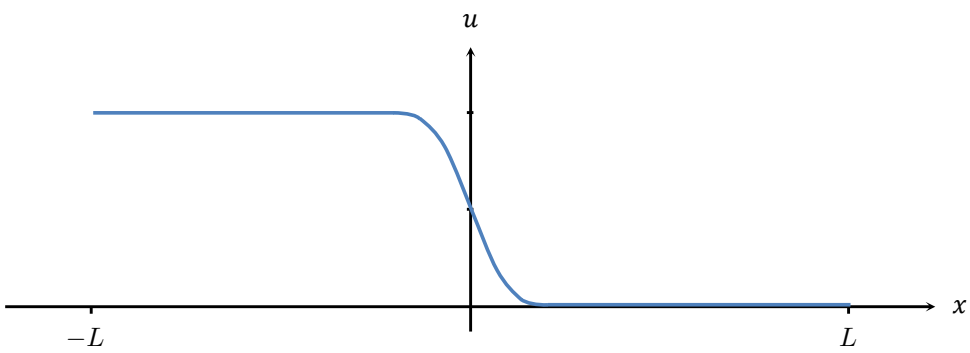

Figure 3.1: Travelling wave solution.

The solution then evolves with time and the travelling wave propagates towards the boundary at L. After a duration of time, it is required that we implement a shift (Figure 3.2). To do this, we start by measuring the distance to which the wave has propagated from its initial position, acknowledging the fact that the travelling wave profile may be converging to a specific form. Subsequently, we take measurements from the centre of the wave, as it is the only point associated to having a u value of 0.5 throughout the simulation. This is done via the use of interpolation, where the central distance x_c is obtained. Using this value, we can approximate a shift relative to the discretised spacial domain.

The approximated shift is given by $N\Delta x$, where N is obtained upon rounding down $\dfrac{x_c}{\Delta x}$ to an integer. We can now modify the vector u corresponding to the solution by eliminating the first N terms, where a spacing of Δx was induced between nodes (see Figure 3.3). Furthermore, we can add N terms to the end of the vector u with values equal to zero. After such modifications, the travelling wave profile is approximately mapped to the centre of the spacial domain, after which the explicit scheme may resume in its computations. Before solving upon iterations, it is required that we shift

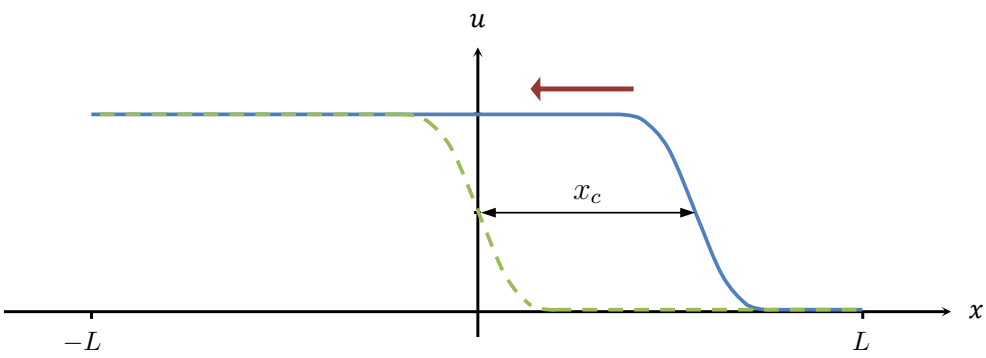

Figure 3.2: Shifting of a travelling wave from its current position (blue) to its updated position (green), where the red arrow represents the direction of shift.

the wave profile to its correct location along the spacial domain for plotting (Figure 3.4).

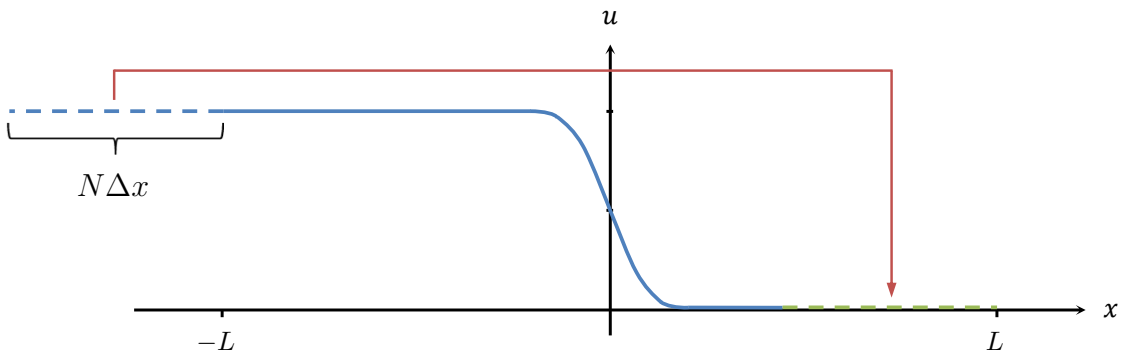

Figure 3.3: Modifying the travelling wave front.

In order to achieve this, we introduce a *cumulative shift*, which represents the accumulated shifts of $N\Delta x$ that are computed after each occurrence of a shift. The spacial domain and the frame of reference are then temporarily shifted by a quantity given by the cumulative shift, yielding the travelling wave profile to be centred as it propagates upon preview.

The speed c of the travelling wave can be determined by averaging the intermittent speeds calculated between every shift. The speed between shifts are calculated by dividing the displacement x_c with the time incurred for the wave to propagate the distance x_c. The code to simulate a travelling wave and to obtain its speeds of propagation can be found in appendix A.1.

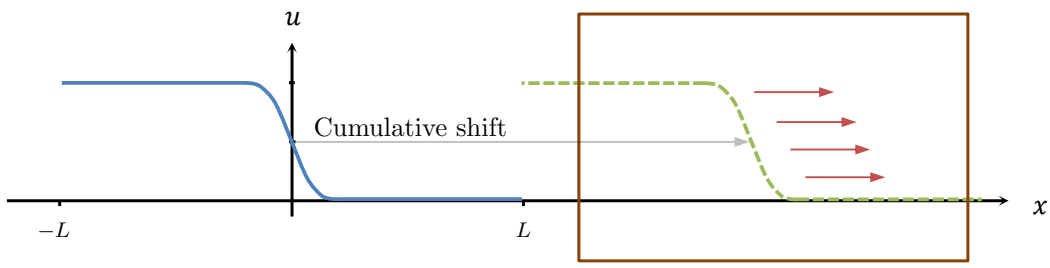

Figure 3.4: Propagating wave front (green) with viewpoint relative to moving wave (brown).

3.2.2 Numerical Solutions

Upon covering the method involved to simulate a travelling wave, we can test to see whether the method will yield solutions that converge to a specific solution for a given k, m and n. Consider the initial wave profiles depicted in Figure 3.5. The travelling

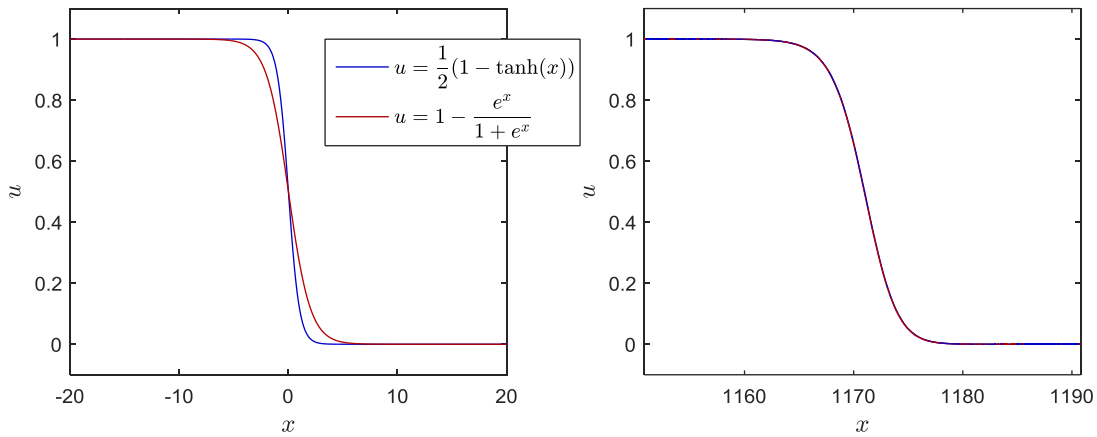

Figure 3.5: Plots illustrating initial wave profiles (left) converging to the same wave profile (right), $k = m = n = 1$, $c = 1.951646563$, $\Delta x = 0.1$, $\Delta t = 0.005$.

wave profiles approximately converged to the same profile with the same propagation speed after a set duration of time. In fact, a general travelling wave profile that may be used as an initial wave profile will converge to the same profile depicted to the right of this figure. The same results can be achieved for a varied k, m and n with the difference of the initial wave profiles converging to a different unique wave profile with a defined speed c. In the set-up depicted in the figure, the solutions converged to a wave profile with an approximate speed of $c \approx 1.951646563$ (Figure 3.6). We can

obtain a more accurate approximation of the unique speed associated to the converged solution by decreasing Δx and Δt (see Table 3.1).

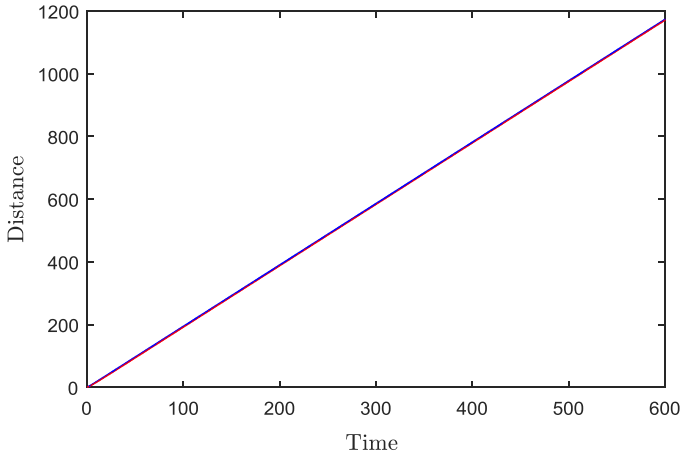

Figure 3.6: Plots depicting the distance covered against time for the travelling wave profiles, with $c \approx 1.951646563$.

Table 3.1: Speeds of the travelling wave with respect to varying Δx and Δt.

Δx	Δt	c
0.125	0.0077	1.941587613
0.1	0.005	1.951646563
0.05	0.0012	1.963284491
0.015	0.000111375	1.966401441
0.01	0.0000495	1.966590289

The speeds appear to be converging to an upper bound of approximately 2 as Δx, $\Delta t \to 0$. This raises questions to whether there exist a unique solution associated to having a unique speed c for every k, m and n. We shall investigate this concept further in a later section.

We will now turn to a more refined analysis based on the effects of varying the parameters k, m and n. A systematic approach will be taken where parameters will be fixed with the exception of a single parameter. Δx, Δt and the duration of time T,

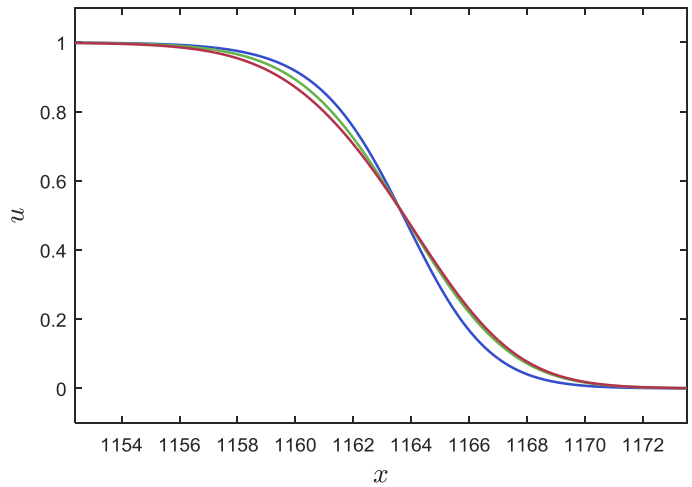

Figure 3.7: Travelling wave solutions with $k = 1$ (blue), $k = 3$ (green) and $k = 6$ (red).

will be set to 0.95, 0.1, 0.048 and 600 seconds respectively, unless stated otherwise. Consider a variation in the parameter k (See Figure 3.7).

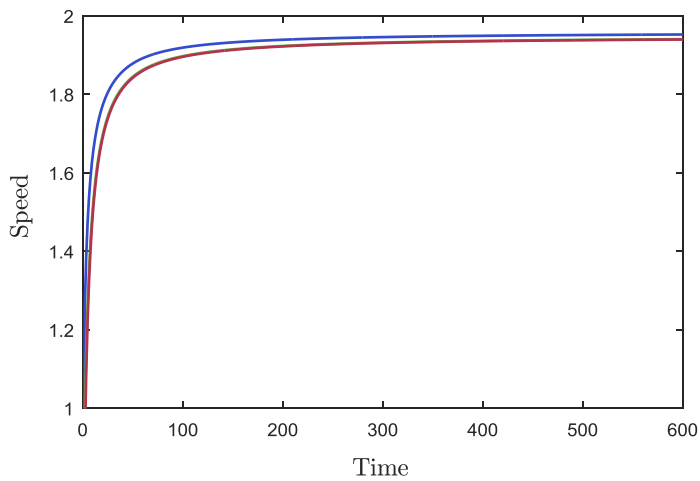

Figure 3.8: Distance time graphs for varying k with $c = 1.952346101$ (blue), $c = 1.940404254$ (green) and $c = 1.939579819$ (red).

We can see that for increasing k, the travelling wave becomes less steep with a very slight decrease in its speed (Figure 3.8). Furthermore, we can observe that the speeds of the waves converged to approximate values as time increased. This is expected, as the numerical scheme produces approximate travelling wave solutions that converge to a specific profile, with a specific speed, as $t \to \infty$. In fact, this phenomenon occurs independently of k, and can be seen to occur for any parameter setting. Consider a

variation in the parameter m (Figure 3.9). There is a noticeable change in the form

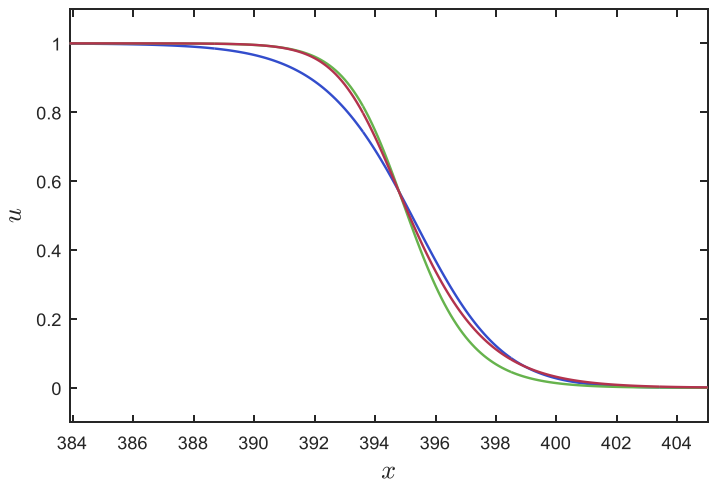

Figure 3.9: Travelling wave solutions with $m = 1$ (blue), $m = 3$ (green) and $m = 6$ (red).

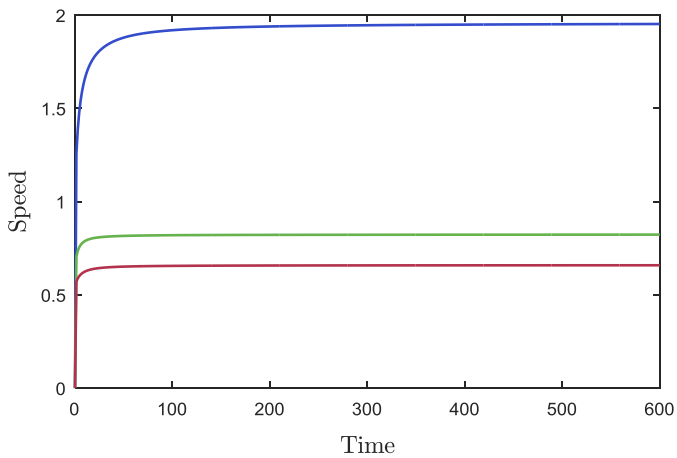

Figure 3.10: Distance time graphs for varying m with $c = 1.952346101$ (blue), $c = 0.822798147$ (green) and $c = 0.658548899$ (red).

of the travelling wave with respect to increasing m. Also, there seems to be difficulty in establishing a relation between the shape of the wave with regards to a change in m. The reason for this is associated to the fact that the PDE under consideration is non-linear, resulting in results that may not agree with intuition. However, we can see that the speed of the travelling wave diminishes at a considerable rate for increasing m. This is evident in Figure 3.10, where the speed of the wave reaches a minimum of $c = 0.658548899$ for $m = 6$. The variable in u associated to having an exponent in m

appears in the polynomial term present in (3.1). Since $0 < u < 1$, an increase in m will correspond to a decrease in the values associated to this polynomial term. Thus, the polynomial term will reduce to a form given by $\epsilon(1-u^n)$ where ϵ is a vector associated to having small entries . As such, we can pose a statement, that there exists a relation between the speed of the travelling wave and with the magnitude of the polynomial term. We shall now consider a variation in the parameter n.

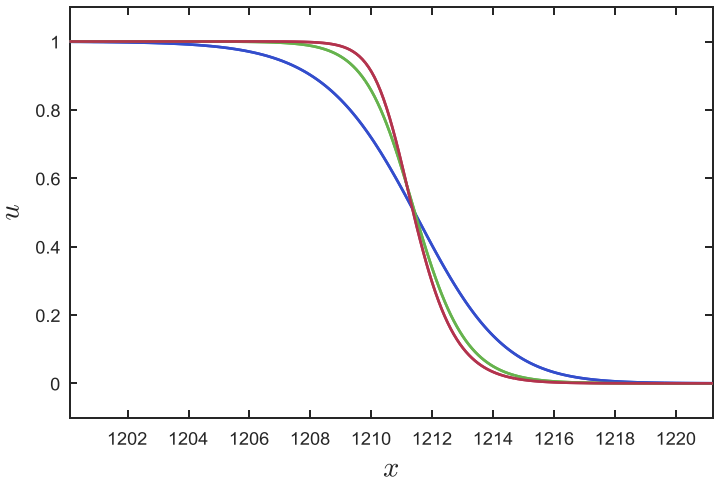

Figure 3.11: Travelling wave solutions with $n = 1$ (blue), $n = 3$ (green) and $n = 6$ (red).

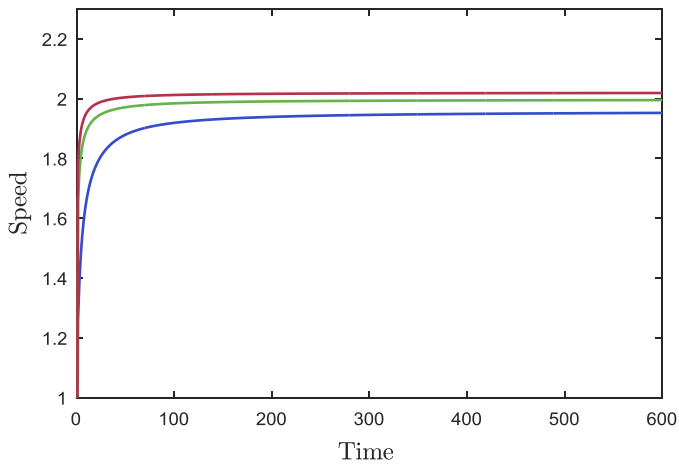

Figure 3.12: Distance time graphs for varying n with $c = 1.952346101$ (blue), $c = 1.995200538$ (green) and $c = 2.018948878$ (red).

The travelling wave present in (3.11) becomes steeper for increasing n. Moreover, we can see that the speed of the wave increases for increasing n, with $c = 2.018948878$

at $n = 6$ (Figure 3.12). Upon increasing n further, the speed of the wave converges to a value of $c \approx 2.05$. The parameter n appears in the polynomial term present in (3.1). For large n, the polynomial term reduces to a form given by $u^m(1-\epsilon)$. Thus, the magnitude of the polynomial term will converge to a fixed state for increasing n. Hence, we can also state that the speed of the wave will converge to a fixed state, given numerically by $c \approx 2.05$. This concludes our investigation towards analysing the effects of varying the parameters, have on the travelling wave. In the next section, the Burgers-Huxley equation (3.1) will be solved analytically.

3.3 Analytical Solution

The Burgers-Huxley equation (3.1) has been shown to fail a test known as the Painlevé test [19], and thus cannot be solved exactly. However, we shall seek to solve for a special set of solutions, with the aid of the factorization method.

To restate for clarity, consider the Burgers-Huxley equation given by,

$$\frac{\partial u}{\partial t} + u^k \frac{\partial u}{\partial x} = \frac{\partial^2 u}{\partial x^2} + u^m \left(1 - u^n\right). \tag{3.11}$$

We initialise by setting $u(x,t) = U(z)$ with $z = p(x - ct)$. Substituting this transformation into the PDE gives,

$$-cp\frac{dU}{dz} + pU^k \frac{dU}{dz} = p^2 \frac{d^2U}{dz^2} + U^m \left(1 - U^n\right). \tag{3.12}$$

It is required that we rearrange the equation in (3.12) to take a suitable form as that present in (2.27). Thus on rearranging (3.12), we obtain

$$\frac{d^2U}{dz^2} + \frac{1}{P}\left(c - U^k\right)\frac{dU}{dz} + \frac{U^m}{p^2}\left(1 - U^n\right) = 0. \tag{3.13}$$

Let $G(U) = \frac{1}{p}(c - U^k)$ and $F(U) = \frac{U^m}{p^2}(1 - U^n)$. From here, we can rearrange the expression for $F(U)$ to get

$$\frac{F(U)}{U} = \frac{U^{m-1}}{p^2}\left(1 - U^n\right) = f_1 f_2, \tag{3.14}$$

where f_1 and f_2 are set to being

$$f_1 = \frac{a\left(1 - U^n\right)}{p}, \; f_2 = \frac{U^{m-1}}{pa}, \tag{3.15}$$

with $a \in \mathbb{R} \setminus \{0\}$. We now substitute the expressions for f_1, f_2 from (3.15) and of $G(U)$ into (2.33) giving,

$$\frac{df_1}{dU}U + f_1 + f_2 = \frac{-anU^n}{p} + \frac{a\left(1-U^n\right)}{p} + \frac{U^{m-1}}{ap} = -\frac{1}{p}\left(c - U^k\right). \tag{3.16}$$

Multiplying equation (3.16) by p and rearranging gives,

$$-anU^n + a - aU^n + \frac{U^{m-1}}{a} + c - U^k = 0. \tag{3.17}$$

At this stage, it is required that we factorise the equation in (3.17). The factorisation method becomes difficult to implement, since the equation is attributed to having three variables, n, m and k, present in the exponent of the variables in U. In order to overcome this ambiguity, we set $n = m - 1 = k = b$ where $b \geq 1$. Thus, we can continue with our derivation, exploiting the process associated with the method. Applying the stated substitutions for m, n and k into equation (3.17), leads to

$$-abU^b + a - aU^b + \frac{U^b}{a} + c - U^b = 0. \tag{3.18}$$

We can now amalgamate like terms, yielding

$$\left(-ab - a + \frac{1}{a} - 1\right)U^b + a + c = 0. \tag{3.19}$$

Since U is not constant, we look for non-trivial solutions by equating the coefficients of U^b and U^0 to zero. We then solve the resulting equations for the variables a and c to get,

$$a = \frac{-1 \pm \sqrt{5+4b}}{2(b+1)}, \ c = -a. \tag{3.20}$$

From the relations present in (3.20), it can be seen that the speed c is indirectly related to the variable b. To this end, it is expected that an increase in b, relative to m, n, and k, will correspond to a decrease in the velocity of the travelling wave.

We can now continue and implement the Cornejo-Pérez grouping technique defined in (2.32) with,

$$f_1 = \frac{a\left(1-U^b\right)}{p}, \ f_2 = \frac{U^b}{ap},$$

after which we obtain

$$\frac{d^2U}{dz^2} - \left[\frac{a\left(1-U^b\right)}{p} + \frac{U^b}{ap} - \frac{abU^b}{p}\right]\frac{dU}{dz} + f_1 f_2 U = 0. \tag{3.21}$$

As state previously, this structure allows us to adopt a factorisation of the form $[D - f_2][D - f_1] = 0$, to get

$$\left[D - \frac{U^b}{ap}\right]\left[D - \frac{a\left(1 - U^b\right)}{p}\right]U = 0. \tag{3.22}$$

Looking at equation (3.22), it can be stated that equation (3.21) will be related to the ODE given by

$$\frac{dU}{dz} \pm \frac{a\left(1 - U^b\right)U}{p} = 0. \tag{3.23}$$

Hence, solving the first order ODE present in (3.23) will bring upon special solutions to the Burgers-Huxley equation. Also, a slight modification has been introduced to equation (3.23), where a $\pm$ sign has been added to the front of a, in order to complement the $\pm$ sign defined in a at (3.20). This is required for equation (3.23) to be satisfied, as $\frac{dU}{dz}$ is a negative quantity, taking into consideration the structure of the travelling wave. Furthermore, equation (3.23) is separable and can be solved explicitly. Hence, equation (3.23) becomes,

$$\int \frac{dU}{\left(1 - U^b\right)U} = \int \mp\frac{a}{p}\,dz. \tag{3.24}$$

Using Maple, we can integrate (3.24) to get,

$$\frac{\ln\left(U^b\right)}{b} - \frac{\ln\left(U^b - 1\right)}{b} = \mp\frac{az}{p} + c_1, \tag{3.25}$$

where c_1 is a constant of integration. In order to avoid discontinuity, the argument of the second logarithmic term will be set to $1 - U^b$ instead of $U^b - 1$, since $0 < U < 1$. Now, to rearrange the expression in (3.25), we obtain

$$\ln\left(\frac{U^b}{1 - U^b}\right) = \mp\frac{azb}{p} + c_1 b. \tag{3.26}$$

After some rearrangement, equation (3.26) can be reformulated to

$$U^b + U^b \exp\left(\mp\frac{azb}{p} + c_1 b\right) = \exp\left(\mp\frac{azb}{p} + c_1 b\right). \tag{3.27}$$

Rearranging for U^b in (3.27) gives,

$$U^b = \frac{\exp\left(\mp\frac{azb}{p} + c_1 b\right)}{1 + \exp\left(\mp\frac{azb}{p} + c_1 b\right)}. \tag{3.28}$$

The equation in (3.28) can be reduced to a simpler form with the aid of introducing a substitution for clarity. The substitution is given by

$$s = \exp\left(\mp\frac{azb}{p} + c_1 b\right).$$

Hence, (3.28) becomes

$$U^b = \frac{s}{1+s} = 1 - \frac{1}{1+s} = 1 - \frac{1}{1+\exp\left(\mp\frac{azb}{p} + c_1 b\right)}, \tag{3.29}$$

resulting in U to be defined as,

$$U(z) = \left[1 - \frac{1}{1+\exp\left(\mp\frac{azb}{p} + c_1 b\right)}\right]^{1/b}. \tag{3.30}$$

We can now implement the inverse transformation of $U(z) = u(x,t)$ with $z = x - ct$, to get

$$u(x,t) = \left[1 - \frac{1}{1+\exp\big(\mp a(x-ct)b + c_1 b\big)}\right]^{1/b}. \tag{3.31}$$

Here, we have a solution defined for every $b > 0$. The special solution given in (3.31) satisfies the boundary conditions imposed in this thesis; that is, for $x \to \pm\infty$, $u \to 0, 1$. However, it is required that we refine the solution to suit the qualitative behaviour of a travelling wave that moves towards the right of the spacial domain in x. As such, we require the parameter $c > 0$. Since $c = -a$, we take the negative sign in a, giving

$$u(x,t) = \left[1 - \frac{1}{1+\exp\big(a(x-ct)b + c_1 b\big)}\right]^{1/b}, \; a = \frac{-1-\sqrt{5+4b}}{2(b+1)}, \tag{3.32}$$

where the constant c_1 relates to an initial shift of the wave, if desired. Such a solution allows for the validation of the explicit scheme. This concept shall be covered in the next section.

3.3.1 Validation of Scheme

To perform a validation of the scheme, the absolute errors between the exact solution and the numerical solution have been computed, where Δx or Δt were fixed, with the

variation of the other. The variable b was set to 1, corresponding to $k = 1$, $m = 2$ and $n = 1$. The simulations ran for a duration of $T = 40$ in between increments of Δt or Δx. The parameters Δt and Δx were set to 0.00019 and 0.15 respectively, when fixed.

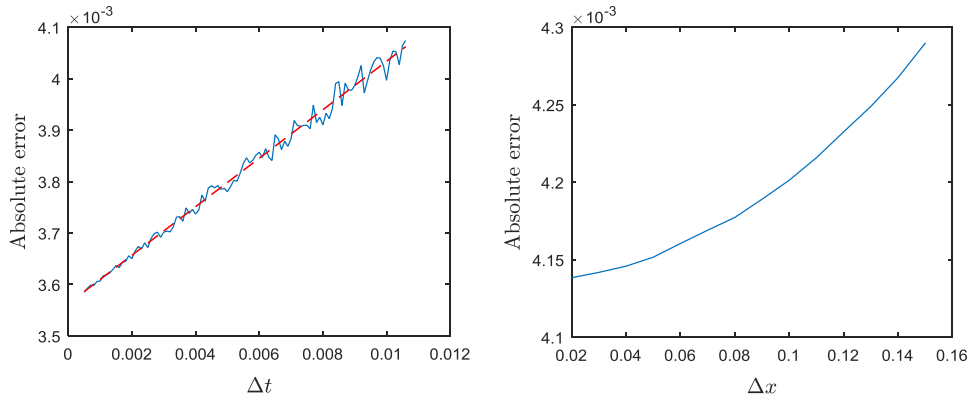

Figure 3.13: Absolute errors associated to differencing the numerical and exact solution for increasing Δt (left) and Δx (right).

We can observe from Figure 3.13, that the absolute error increases at a very small rate for increasing Δt or Δx. Moreover, it is apparent that absolute error does not grow without bound. Hence, we can confirm that the numerical scheme is valid.

We shall now shift our focus towards investigating the existence and dynamics of solutions, by conducting a phase plane analysis. This concept will be explored in the following section.

3.4 Phase Plane Analysis

There are many non-linear PDEs that do not have analytical solutions at this present time, and thus require alternative means for studying for their dynamics. Phase plane analysis provides an excellent means for studying the qualitative behaviour of dynamical systems, attributed to such equations. Furthermore, we can employ this technique to obtain information based on the stability of the system, and to provide further insight on the existence of solutions. By way of illustration of the technique involved,

consider the Burgers-Huxley equation defined in (3.1), as

$$u_t + u^k u_x = u_{xx} + u^m(1 - u^n). \tag{3.33}$$

We start by setting $f(u) = u^m(1 - u^n)$. Based on the parameters involved in $f(u)$, we can establish two general forms for $f(u)$, based on specific parameter settings (Figure 3.14). Since $f(u)$ varies for different parameter settings, the following properties

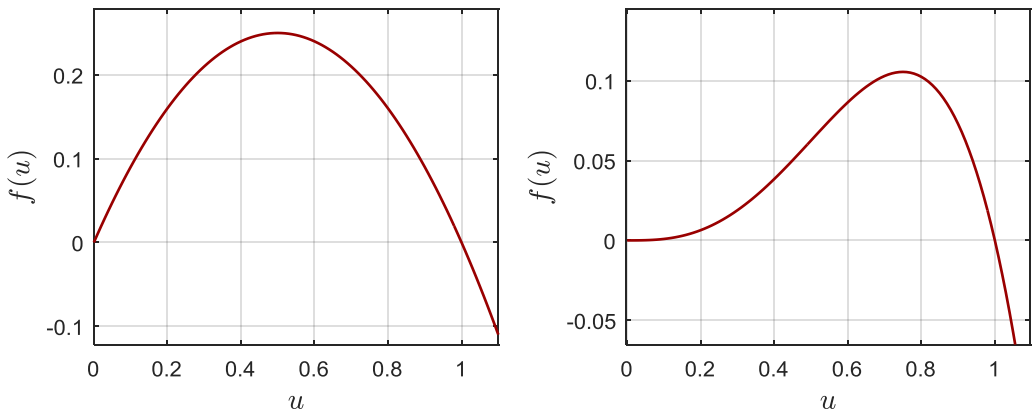

Figure 3.14: General forms of $f(u)$ with $n \geq 1$ and $m = 1$ (left), $n \geq 1$ and $m > 1$ (right).

associated to $f(u)$, independent of such parameters, can be identified: $f(0) = f(1) = 0$, $f > 0$ on $u \in (0, 1)$, $f < 0$ on $u > 1$ and $f' < 0$ at $u = 1$. When considering the parameters involved, we have $f'(0) > 0$ for $m = 1$ and $f'(0) = 0$ for $m > 1$.

In order to determine the stability of the constant solutions, we linearise at $u = 0, 1$. Thus, we taylor expand $f(u)$ at $u = a$ to get,

$$f(u) = f(a) + f'(a)u + \dots$$

Thus, for $m = 1$, the constants $u = 0$ and $u = 1$ are unstable and stable solutions respectively. For $m > 1$, we have stable solutions at $u = 1$ and $u = 0$. We shall now introduce a travelling wave solution of the form:

$$u(x, t) = v(x - ct) = v(z), \tag{3.34}$$

where c is the velocity of the wave. Hence, $u_x = v', u_{xx} = v''$ and $u_t = -cv'$ where $' = \frac{d}{dz}$.

In order for v to be a solution to the problem, it is required that the ansatz v satisfies the ODE given by,

$$-cv' + v^k v' = v'' + f(v). \tag{3.35}$$

The boundary conditions are,

$$u \to 1 \;\; as \;\; x \to -\infty, \, u \to 0 \;\; as \;\; x \to \infty.$$

These conditions transform to

$$\lim_{z\to-\infty} v(z) = 1, \lim_{z\to\infty} v(z) = 0, \lim_{z\to\pm\infty} v'(z) = 0. \tag{3.36}$$

Using (3.35) and (3.36), we can conduct a phase plane analysis. Setting $w = v'$, equation (3.35) reduces into two first-order ODEs given by,

$$\begin{aligned} v' &= w \\ w' &= v^k w - cw - f(v). \end{aligned} \tag{3.37}$$

Furthermore, the conditions in (3.36) can be expressed in a more compact form as

$$\lim_{z\to-\infty} (v, w) = (1, 0), \lim_{z\to\infty} (v, w) = (0, 0).$$

The system in (3.37) has critical points at $(1, 0)$ and $(0, 0)$. In order to determine the stability of these points, it is required that we linearise the system present in (3.37). As such, the Jacobian matrix associated to the linearised system is expressed as,

$$J = \begin{pmatrix} 0 & 1 \\ kv^{k-1}w - f'(v) & v^k - c \end{pmatrix}. \tag{3.38}$$

From here, we can obtain the characteristic equation defined as,

$$\det(J - \lambda I), \tag{3.39}$$

where λ is an eigenvalue associated to the system at a critical point. The characteristic equation is given by,

$$\begin{vmatrix} -\lambda & 1 \\ kv^{k-1}w - f'(v) & v^k - c - \lambda \end{vmatrix} = -\lambda(v^k - c - \lambda) - kv^{k-1}w + f'(v) = 0. \tag{3.40}$$

Simplifying (3.40) gives,

$$\lambda^2 + (c - v^k)\lambda + f'(v) - kv^{k-1}w = 0. \tag{3.41}$$

For the critical point $(1, 0)$, equation (3.41) becomes,

$$\lambda_1^2 + (c - 1)\lambda_1 + f'(1) = 0.$$

Solving for the eigenvalues $\lambda_1^{\pm}$ gives,

$$\lambda_1^{\pm} = \frac{-(c-1) \pm \sqrt{(c-1)^2 - 4f'(1)}}{2}. \tag{3.42}$$

We can obtain the eigenvectors associated with the eigenvalues by solving

$$(A - \lambda I)\mathbf{v} = 0, \tag{3.43}$$

where A is the coefficient matrix defined in (3.38), evaluated at the stationary point. Thus, the equations corresponding to the eigenvectors associated to $\lambda_1^{\pm}$ are given by,

$$w = \lambda_1^{\pm}(v - 1). \tag{3.44}$$

Since $f'(1) < 0$ for $m \geq 1$, the point $(1, 0)$ can be classified as being a saddle node for $m \geq 1$. Similarly, to classify the critical point $(0, 0)$, equation (3.41) becomes

$$\lambda_2^2 + c\lambda_2 + f'(0) = 0. \tag{3.45}$$

Thus, from equation (3.45), we can solve for the eigenvalues $\lambda_2^{\pm}$, giving

$$\lambda_2^{\pm} = \frac{-c \pm \sqrt{c^2 - 4f'(0)}}{2}. \tag{3.46}$$

Using (3.43), the equations representing the eigenvectors are

$$w = \lambda_2^{\pm} v. \tag{3.47}$$

For $m = 1$, we have $f'(0) > 0$ and the stability of the stationary point depends on the discriminant $c^2 - 4f'(0)$. To be more specific, we have $f'(u) = mu^{m-1} - (m+n)u^{m+n+1}$. Thus, for $m = 1$, $f'(0) = 1$, and the point $(0, 0)$ is a stable node for $c \geq 2$ and a stable focus for $0 < c < 2$. As for $m > 1$, we have $f'(0) = 0$, yielding an eigenvalue equal to zero. As a result, we have a non-hyperbolic point and we cannot determine the stability of the point $(0, 0)$ through linearisation. It would require that we include

additional non-linear terms to classify the point, which is beyond the scope of our investigation within this thesis. However, upon observations of the phase portraits associated with $m > 1$, we can determine the dynamics surrounding the point thereof. Thus, we shall investigate the system further through the analysis of phase portraits. The phase portraits will be developed in MATLAB using a program known as *pplane* [1]. The parameters n and k will be set to 1, as the dynamics of solutions remain the same for $k, n \geq 1$. We will start by investigating the dynamics of the system for two cases, namely for setting $m = 1$ and then for setting $m > 1$. As for the phase portraits, the stable and unstable orbits associated with the critical point $(1, 0)$, will be given by green and red curves respectively. The trajectories and stationary points will be given by blue curves and black dots where appropriate.

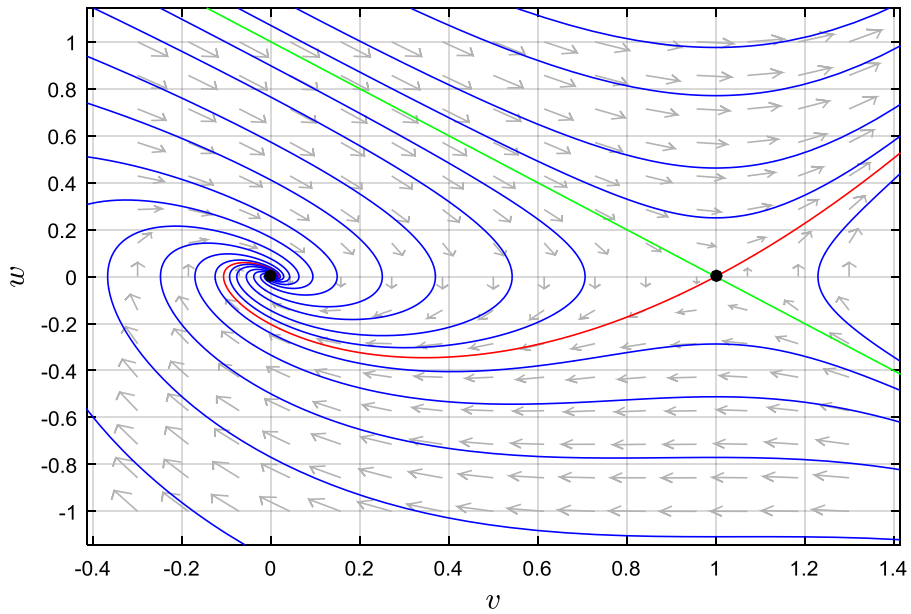

Figure 3.15: Phase portrait with $m = 1$, $0 < c < 2$, spiral focus at $(0, 0)$ and a saddle node at $(1, 0)$.

In order for a travelling wave to exist, it is required that $v(z)$ approaches constant states as $z \to \pm\infty$. In other words, it is required that the two ends of a trajectory meet at fixed points. From the phase portrait depicted in Figure 3.15, we can see that a trajectory emitting from the point $(1, 0)$, spirals inwards towards $(0, 0)$. The wave solution corresponding to this trajectory satisfies the boundary conditions. However, such a solution violates the condition that $0 < u < 1$. This is illustrated in Figure

3.16, where oscillations are observed as $x \to \infty$.

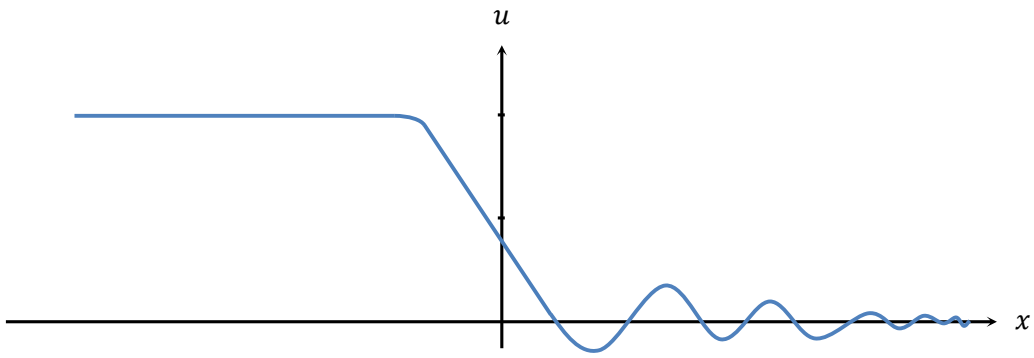

Figure 3.16: Wave solution with oscillatory behaviour.

Hence, for $0 < c < 2$, there does not exist a travelling wave solution that satisfies the conditions imposed. On the contrary, consider the general form of a phase portrait with setting $c \geq 2$ (Figure 3.17). There appears to be a heteroclinic orbit connecting

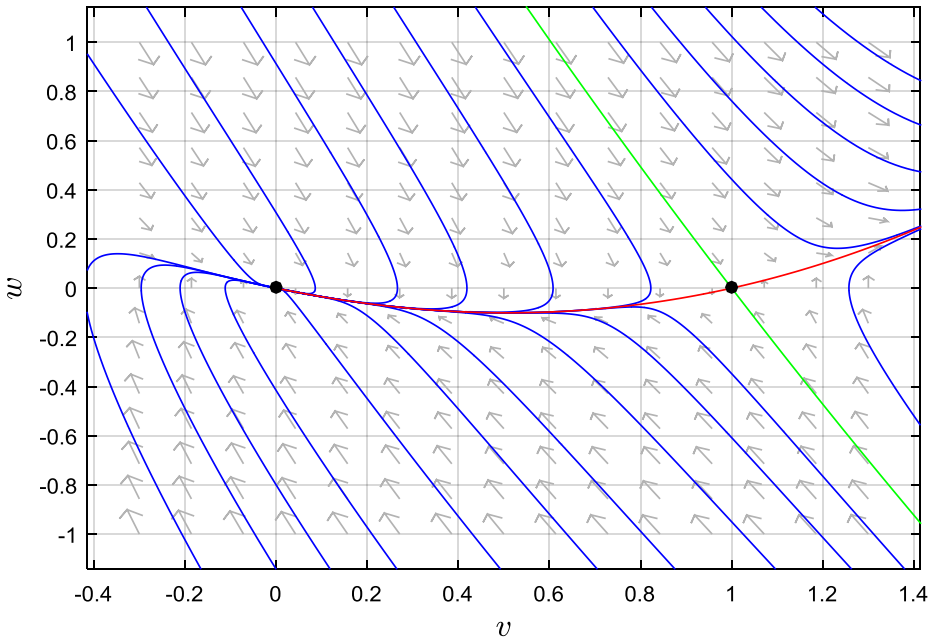

Figure 3.17: Phase portrait with $m = 1$, $c = 3$, stable node at $(0, 0)$ and a saddle node at $(1, 0)$.

the stationary points $(0, 0)$ and $(1, 0)$. This is true for a general $c \geq 2$. Moreover, the numerical solutions converged to a specific wave with speed $c \approx 2$. This sheds light on the existence of wave solutions, considering the set parameters, as we can

observe that there may not be a unique wave solution with a particular speed of 2. At a later stage, we shall investigate this concept further, where we shall derive a power series approximation of an equation that will model a heteroclinic orbit associated to a feasible travelling wave solution. The existence of such an equation will depend primarily on the possible speeds c to which there may exist a travelling wave.

Consider an increase in the parameter m, where the speed c has been set to a small value. It is apparent from Figure 3.18 that a travelling wave solution does not exist

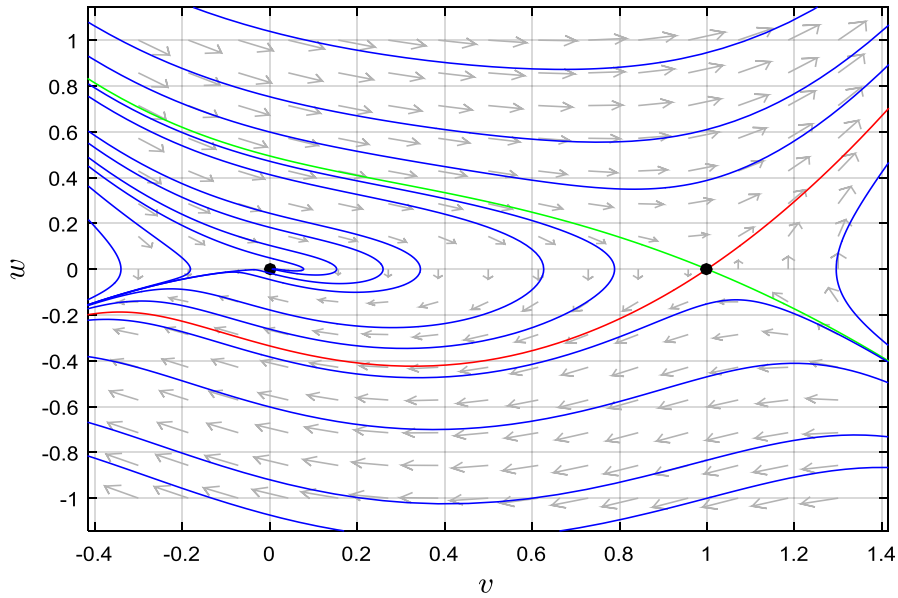

Figure 3.18: Phase portrait with $m = 2$, $c = 0.5$ and a saddle node at $(1, 0)$.

for $c = 0.5$. Such a result is true for $0 < c < c^*$, where c^* is some critical value. The trajectory emitting from the stationary point at $(1, 0)$ exits the visual domain, which translates to a solution u with no defined limit in space for $x \to \infty$. Upon increasing c, the trajectory approaches the stationary point at the origin, after which a feasible travelling wave solution is observed for $c = c^*$ (Figure 3.19).

The form of the heteroclinic orbit is unique with $c^* = 1$, for setting $m = 2$. Upon increasing m, it is observed that the critical value c^* decreases, to which a travelling wave solution exists. The relation between m and c^* may be established if we were to pursue an investigation towards classifying the stationary point at $(0, 0)$ with the addition of the non-linear terms that were neglected upon linearisation. A further

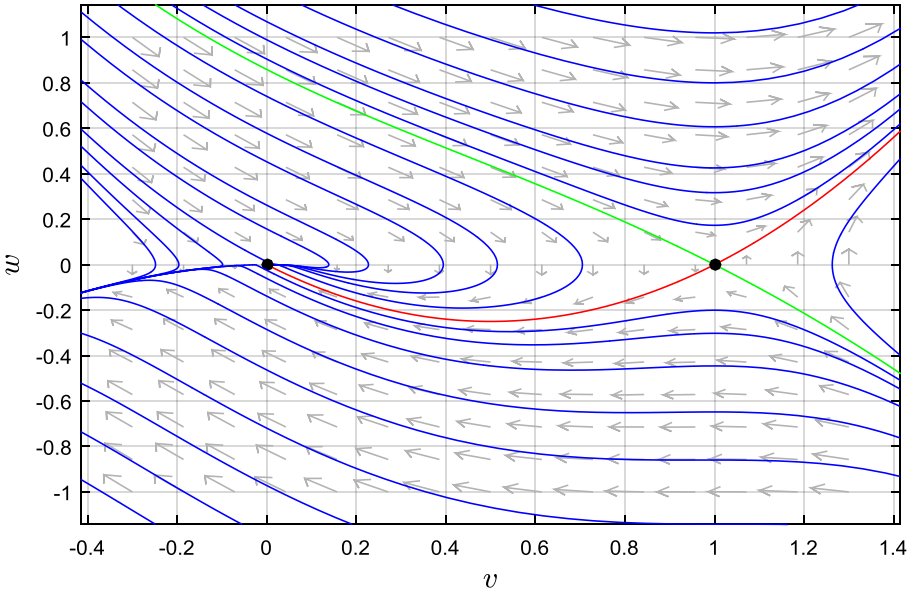

Figure 3.19: Phase portrait with $m = 2$, $c = c^* = 1$ and a saddle node at $(1, 0)$.

increase in c with $c > c^*$, results in a deformation of the heteroclinic orbit depicted with $c = c^*$. The form of the trajectory is shown in Figure 3.20, where a noticeable skewness is observed as $v \to 0$.

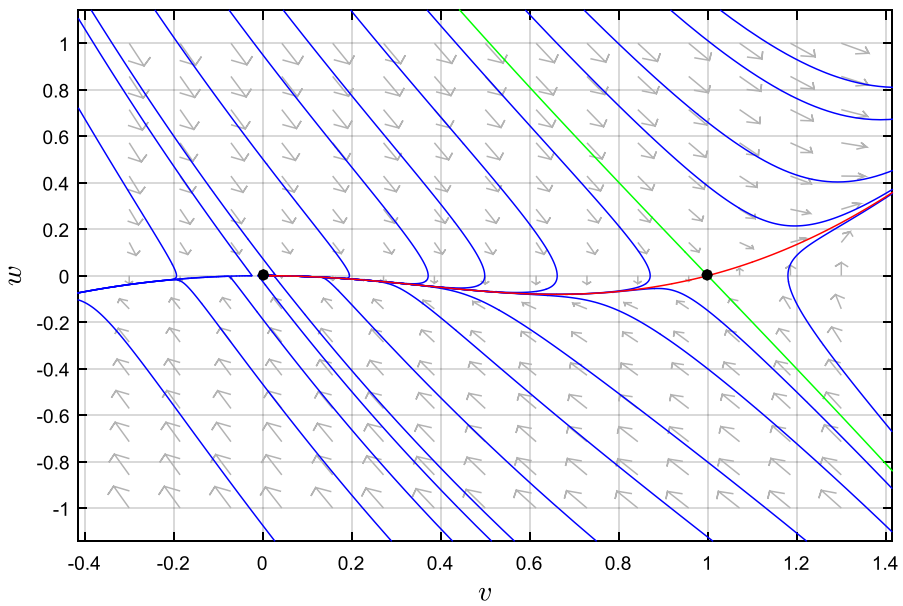

Figure 3.20: Phase portrait with $m = 2$, $c = 2.5$ and a saddle node at $(1, 0)$.

The trajectory appears to be a heteroclinic orbit, which satisfies all conditions. Such

a solution is visible for increasing c further. Hence, for further insight on the existence of solutions, we shall model the heteroclinic orbits with the use of power series approximations.

3.4.1 Power Series Approximations of Heteroclinic Orbits

In order to obtain an equation that approximates the trajectory passing from $(0, 0)$ to $(1, 0)$, we make use of a power series approximation of the form,

$$w(v) = \sum_{s=0}^{\infty} a_s v^s. \tag{3.48}$$

where a_s are constants to be solved for. The vector field of $w(v)$ is defined upon solving $\frac{dw}{dv}$. From (3.37), we get,

$$\frac{w'}{v'} = \frac{dw}{dz}\frac{dz}{dv} = \frac{dw}{dv}. \tag{3.49}$$

Hence, evaluating (3.49) gives,

$$\frac{dw}{dv} = \frac{-cw + v^k w - v^m(1 - v^n)}{w}. \tag{3.50}$$

We can rearrange (3.50) to obtain

$$w\frac{dw}{dv} + cw - v^k w + v^m(1 - v^n) = 0. \tag{3.51}$$

From here, we substitute the power series given in (3.48) into (3.51) to get

$$\left(\sum_{s=0}^{\infty} a_s v^s\right)\left(\sum_{s=0}^{\infty} s a_s v^{s-1}\right) + c\sum_{s=0}^{\infty} a_s v^s - \sum_{s=0}^{\infty} a_s v^{s+k} + v^m(1 - v^n) = 0. \tag{3.52}$$

Using this expression, we can obtain sets of equations after equating the coefficients of the variables in v^s, where $s > 1$, to zero. To find the particular approximate equation corresponding to the heteroclinic orbit, we use the boundary conditions. We have $w(0) = 0$, resulting in $a_0 = 0$ in (3.48). The system of equations are then solved to obtain expressions for the remainder of the coefficients a_s, where $s > 1$, in terms of c. At this stage, we introduce the second boundary condition of $w(1) = 0$, where an additional equation is generated, given by

$$a_1 + a_2 + \ldots + a_s = 0. \tag{3.53}$$

Upon solving this equation, we obtain roots representing the values to which c can take for an approximate power series solution to be generated. However, It should be noted that some of the solutions in c do not yield power series solutions that model a feasible travelling wave. This is due to the fact that the condition $w(1) = 0$, resulting in equation (3.53), is true for $s \to \infty$. Since we are dealing with a finite number of terms in s, the condition introduces a slight error, resulting in power series approximations that do not model a heteroclinic orbit correctly. Such solutions in c will be omitted from results obtained hereof. The code to generate power series solutions of order s can be found in appendix A.4.

We are now in the position to model a heteroclinic orbit associated to a feasible travelling wave solution. We shall start by setting $m = 1$, after which we generate power series approximations of different orders. Such solutions are present in Table 3.2, where a set of interesting results can be observed. Upon increasing the number of terms in the power series approximation, we obtain different sets of speeds c that are unique and vary in magnitude. We can also observe a general correlation between the number of terms and the speeds c, where an increased number of c values are found for increasing the number of terms.

Table 3.2: Travelling wave solutions with corresponding speeds c (given to 4.d.p), obtained upon solving power series approximations of different orders.

Number of terms	Speed c						
3	2.0566	2.5000	4.9434				
4	3.5075	10.2520					
5	2.0390	3.1887	5.4018	18.9243			
6	3.1022	4.2342	8.3531	31.5616			
7	3.0858	3.8259	5.8009	12.4592	48.8183		
8	3.6855	4.8278	7.9417	17.8360	71.3670		
9	3.6501	4.4091	6.1778	10.6913	24.6145	99.8876	
10	3.6457	4.2437	5.3509	7.8975			
11	3.6456	4.1964	4.9514	6.5451	10.0029	42.9398	177.5798

To achieve a more vivid perspective on the results obtained in Table 3.2, a set of data

plots have been produced (Figure 3.21). An interesting phenomenon can be observed to the left of the figure, where the dots corresponding to solutions partake in the formation of structures depicted as dotted curved lines. New dotted curves appear to form as the number of terms are increased. Also, the magnitude of solutions associated to the curves increase with increasing the number of terms. These phenomenon are a direct implication of the very nature behind solving for the power series approximations, where polynomial equations with a variable in c are formed, based on the boundary condition of $w(1) = 0$.

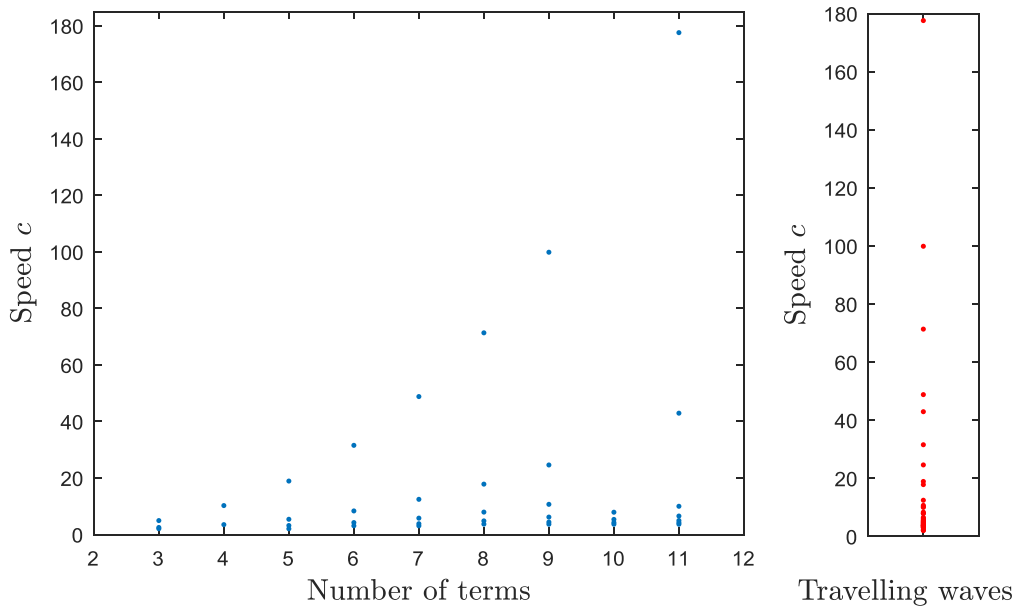

Figure 3.21: Travelling wave solutions with speeds c, obtained upon solving power series approximations for a specific number of terms (left), after which the solutions were combined (right).

From a general perspective, we can see from the right of Figure 3.21, that there are a concentrated number of solutions present near $c = 2$. Furthermore, we can observe a strong correlation between obtaining new solutions in c, with increasing the number of terms of the power series approximation. Based on the analysis conducted, we can pose a strong hypothesis, that there exists an infinite number of travelling wave solutions for $m = 1$ with speeds $c \in [2, M]$, where M is an upper bound on the speed to which a travelling wave solution may exit.

We can now conduct a thorough analysis to examine the properties associated with

the shape of a travelling wave solution, with increasing its speed. Consider the approximate heteroclinic orbits present in Figure 3.22, where power series approximations of order nine were generated.

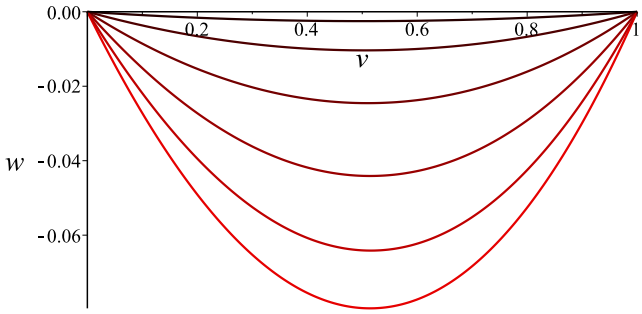

Figure 3.22: Approximate heteroclinic orbits with $m = 1$ for various c values, ranging from a speed $c \approx 3.6501$ (light red), to a higher speed $c \approx 99.8876$ (dark red).

It is shown that the heteroclinic orbits vary in levels of convexity, where an increase in c, results in the trajectory becoming less convex. This attribute can be interpreted as the travelling wave solution becoming less steep for increasing its speed. However, this does not allow for one to come to the conclusion that the steepness of a wave is primarily dictated by its travelling speed, as the system under consideration is non-linear, resulting in other factors that may influence the waves steepness. We can see that the eigenvalues $\lambda_2^{\pm}$ present in (3.46) are dependent on the speed of the wave. The eigenvalues in this context, determine the rate at which a solution decays as $x \to \infty$, which ultimately influences the shape of the wave. Further to this investigation, consider the relation present in Figure 3.23, between the speed c and the eigenvalues $\lambda_2^{\pm}$.

Upon increasing the speed c, we can observe that λ_2^{+} increases towards an upper bound of zero, whilst λ_2^{-} decreases. As a consequence, we can establish that the heteroclinic orbit and most other trajectories are tangential to the eigenvector with equation $w = \lambda_2^{+} v$, given in (3.47), as $v \to 0$. This is due to the fact that trajectories are tangential to the eigenvector corresponding to the eigenvalue with smallest modulus at $(0, 0)$. The gradient of the equation $w = \lambda_2^{+} v$ will increase for increasing c, and thus, the convexity of the heteroclinic orbits will decrease. Furthermore, an increase in λ_2^{+} will correspond to a slower decay in the solution u, as $x \to \infty$. We can obtain

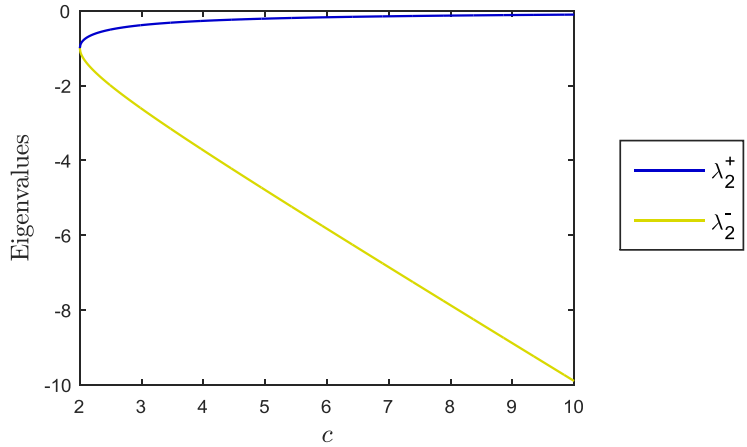

Figure 3.23: Relation between the eigenvalues $\lambda_2^{\pm}$ and an increase in speed for $2 \leq c \leq 10$.

the rate of decay of the wave as $x \to \infty$, upon solving $w = \lambda_2^+$. Hence, we re-express this equation as,

$$v' = \lambda_2^+.$$

This equation is separable and can be solved for to get,

$$v = Be^{\lambda_2^+ x},$$

where B is an arbitrary constant. Therefore, we can conclude that the solution in u, decays exponentially as $x \to \infty$. This analysis gives more of an insight towards the dynamics observed in Figure 3.22.

We shall now shift our focus towards the analysis of travelling wave solutions obtained for setting $m > 1$. It is depicted in Figures 3.19 and 3.20 that we have two different forms of travelling wave solutions. The wave solution with speed $c = c^*$, present in Figure 3.19, exhibits exponential decay as $x \to \infty$. Only one solution of this form is observed for every $m > 1$. Upon emulating the power series method, we obtain a power series approximation of the heteroclinic orbit perceived with $c = c^*$. In order to obtain powers series approximations corresponding to the solution in Figure 3.20, it is required that we choose $a_1 = 0$, where a quadratic equation in a_1 is obtained upon equating the coefficient of v in equation (3.52) to zero. A geometrical interpretation for this reasoning is given as follows. The heteroclinic orbit takes a form of $w = -rv^2$, where $r > 0$, locally near the origin. From the power series approximation, the term $a_1 v$ will dominate as $v \to 0$, since $0 < v < 1$. Hence, we require $a_1 = 0$, resulting in a dominant

term of a_2v^2, as $v \to 0$, and where a_2 is expected to take a negative quantity. As such, we obtain power series approximations that model travelling wave solutions with various speeds. An example of which is illustrated in Figure 3.24, where approximate heteroclinic orbits are generated, for solving a set of power series approximations with thirty terms. The code to generate these power series approximations can be located in appendix A.5.

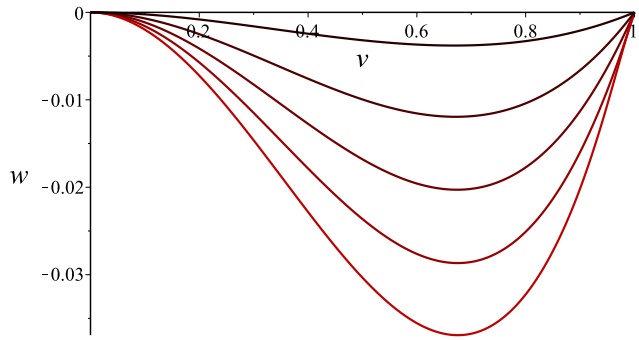

Figure 3.24: Approximate heteroclinic orbits with $m = 2$ for various c values, ranging from a speed $c \approx 4.6864$ (light red), to a higher speed $c \approx 39.7208$ (dark red).

The rate at which the solution u decays as $x \to \infty$ can be obtained upon solving the equation $w = -rv^2$. Thus, we re-express the equation as,

$$v' = -rv^2.$$

This equation is separable and can be solved to get,

$$v = \frac{1}{rx + b},$$

where b is a constant. Hence, the solution decays algebraically as $x \to \infty$, and the wave solution would generally be less steep as compared to a solution with exponential decay for an equivalent set of parameters involved.

Since similar results are observed for setting $m > 1$ with compared to setting $m = 1$, we can pose the same hypothesis, that there exists an infinite number of travelling wave solutions with speeds $c \in [c^*, N]$, where N is an upper limit in the speed to which a travelling wave may exist. This concludes our investigation towards the analysis the Burgers-Huxley equation.

In conclusion, the analysis conducted within this chapter sheds light on the dynamics of the Burgers-Huxley equation, with respect to the parameters k, m and n. The method behind shifting a travelling wave solution was addressed, and solutions depicting the effects of varying the parameters k, m and n were covered. A phase plane analyses was conducted, where qualitative results were obtained. Finally, the existence of travelling wave solutions were comprehended, with the use of power series approximations. In the next chapter, we shall explore the dynamics associated with the FitzHugh-Nagumo equations.

Chapter 4

FitzHugh-Nagumo Equation

The first segment of this chapter focuses on the underlying theory behind the FitzHugh-Nagumo equations, where two similar equations are stated. The chapter then leads onto the investigation of the dynamics of the FitzHugh-Nagumo equations, based on a variation of parameters. This is done numerically. Finally, a singular perturbation method is conducted, in favour of exploring the characteristics associated with the equation further.

The FitzHugh-Nagumo equations have been studied extensively in favour of their applications. The equations are used to model electrical activity in a neuron [25] and are a simplification of the Hodgkin-Huxley model derived in 1952 [7], which is used to model the same phenomenon. An illustration of this is present in Figure 4.1. Furthermore, the applications of the FitzHugh-Nagumo equations extend to developing qualitative descriptions for excitable media on a general basis [20]. The FitzHugh-Nagumo equations are given by,

$$\frac{\partial u}{\partial t} = D\frac{\partial^2 u}{\partial x^2} + f(u) - v, \quad \frac{\partial v}{\partial t} = bu - \gamma v, \tag{4.1}$$

where $f(u) = u(1-u)(u-a)$ and where the parameters D, b, γ and a are positive parameters. The parameter D corresponds to the diffusion coefficient.

The FitzHugh-Nagumo equations are known as an *excitable* system. Such systems are attributed to having a unique attractor with two modes of returning to a rest state. If a small stimulus was introduced, the system would take a short recursion in phase space,

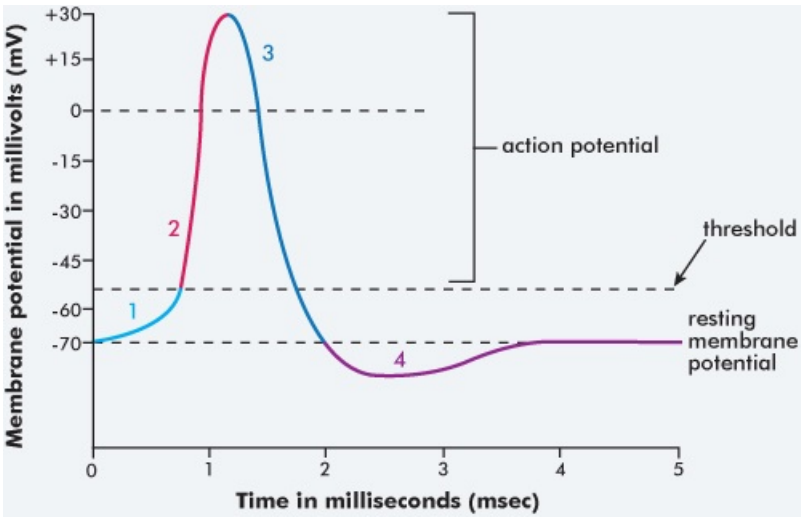

Figure 4.1: Depolarisation and re-polarisation of a neuron, recorded with an oscilloscope [2].

before returning to the equilibrium state. If a large stimulus was initiated, the system would deviate further away, taking a longer path in phase space, before returning to the rest state. Furthermore, the FitzHugh-Nagumo equations are associated with having a *homoclinic orbit* in phase space, which corresponds to a trajectory that joins a saddle node to itself, by emitting from an unstable manifold, to a stable manifold. Due to this structure, we cannot apply a power series approximation to investigate the existence of solutions, as done previously. Furthermore, it would require that we produce three dimensional phase portraits to analyse the FitzHugh-Nagumo equations for their dynamics, where a very limited amount of information can be deduced. Thus we will shift our focus towards a different analysis within this chapter.

There are different equations that resemble the FitzHugh-Nagumo equation present in (4.1), that do have analytical solutions. An example of which is Nagumo's equation, which is given by,

$$u_t = u_{xx} + u\,(1-u)\,(u-a)\,, \tag{4.2}$$

where $0 < a < 1$, and with boundary conditions $u(-\infty, t) \to 1$, $u(\infty, t) \to 0$. This equation is attributed to having a wave front solution, which is of interest, given the FitzHugh-Nagumo equation is associated with having a travelling pulse solution. The Nagumo equation can be solved in the following manner. We start by introducing a travelling wave ansatz of the form

$$u(x,t) = v(z), \tag{4.3}$$

where $z = x - ct$. Upon substituting (4.3) into (4.2), we get

$$-cv' = v'' + v\,(1 - v)\,(v - a)\,. \tag{4.4}$$

From here, we propose a first order ODE that may be compatible with equation (4.2). The ODE is given by,

$$v' = kv(1 - v),\ k \in \mathbb{R}. \tag{4.5}$$

Upon differentiating (4.6), we obtain

$$v'' = kv' - 2kvv' = k^2v(1 - v) - 2k^2v^2(1 - v). \tag{4.6}$$

We now substitute (4.5) and (4.6) into (4.4), yielding

$$-ckv(1 - v) = k^2v(1 - v) - 2k^2v^2(1 - v) + v(1 - v)(v - a). \tag{4.7}$$

Taking expression (4.7), we rearrange and factor out like terms, to get

$$(-2k^2 + 1)v^3 + (ck + 3k^2 - a - 1)v^2 + (-ck - k^2 + a)v = 0. \tag{4.8}$$

In order for the proposed ODE given in (4.5) to satisfy equation (4.4), we require the coefficients of v, v^2, and v^3 to equal zero. Hence, we can solve the resulting equations to obtain the following relations:

$$k = \pm\frac{1}{\sqrt{2}},\ c = k(2a - 1). \tag{4.9}$$

Thus, the ODE given in (4.5) is compatible with equation (4.4), taking into consideration the relations present in (4.9). Therefore, upon solving the first order ODE, we will acquire a solution to the PDE given in (4.2). The ODE in (4.5) is separable and can be integrated directly from a form given by,

$$\frac{dv}{v(1 - v)} = kdz. \tag{4.10}$$

Using Maple to integrate (4.10), gives

$$\ln(v) - \ln(v - 1) = kz + s, \tag{4.11}$$

where s is a constant of integration. To avoid discontinuity, we set the argument of the second logarithmic term to $1 - v$, since $0 < v < 1$. From here, we can rearrange the expression to obtain a solution for v, given by

$$v = \frac{\exp(kz + s)}{1 + \exp(kz + s)} = 1 - \frac{1}{1 + \exp(kz + s)}. \tag{4.12}$$

Furthermore, we can introduce the inverse transformation of $v(z) = u(x,t)$, to obtain an explicit solution to (4.2), with

$$u(x,t) = 1 - \frac{1}{1 + \exp(k(x - ct) + s)}, \tag{4.13}$$

and where s represents an initial shift of the wave. To refine the solution to agree with the natural behaviour of a travelling wave, we consider the direction of propagation, given the boundary conditions of $u(\pm\infty) \to 0, 1$. Thus, from (4.9), we require $k = -\frac{1}{\sqrt{2}}$, with $c > 0$. This particular setting brings upon an additional condition with $0 < a < \frac{1}{2}$. Moreover, the resulting wave will propagate towards the right of the spacial domain with respect to time.

For the interested reader, the FitzHugh-Nagumo equation associated with convection [17], given by

$$u_t + kuu_x - u_{2x} - u(1-u)(a-u) = 0,$$

may also be solved for an exact solution that takes a form of a wave front solution. Such a solution is defined to be

$$u = \frac{\exp\left[1/\sqrt{m})x + ((1-am)/m)t + \delta_1\right] + a\exp\left[(a/\sqrt{m})x + (a(a-m)/m)t + \delta_2\right]}{c + \exp\left[(1/\sqrt{m})x + ((1-am)/m)t + \delta_1\right] + \exp\left[(a/\sqrt{m})x + (a(a-m)/m)t + \delta_2\right]},$$

where m, a, δ_1, δ_2 are parameters. Unfortunately, the FitzHugh-Nagumo equations cannot be solved analytically. Thus, we shall resort to solving the equations numerically in the following section.

4.1 Numerical Results

Before we start to solve the FitzHugh-Nagumo equations numerically, it is required that we derive a fundamental condition associated with the parameters of the equation, for a pulse wave solution to exist. The condition can be obtained as follows. We begin by seeking a solutions of the form $u = U(z) = U(x - ct)$ and $v = V(z) = V(x - ct)$. We then substitute the ansatzes for u and v into the FitzHugh-Nagumo equations in (4.1), to obtain

$$\begin{aligned} -cU' &= DU'' + U(U-a)(1-U) - V, \\ -cV' &= bU - \gamma V. \end{aligned} \tag{4.14}$$

From here, we let $Y = U'$ and $Y' = U''$. Thus, we can express the system in (4.14) as,

$$\begin{aligned} DY' &= -cY - U(U-a)(1-U) + V, \\ U' &= Y, \\ V' &= \frac{\gamma}{c}V - \frac{b}{c}U. \end{aligned} \tag{4.15}$$

Upon evaluation, we can define the critical points as

$$\left(0, U_r, \frac{b}{\gamma}U_r\right), r = 1, 2, 3,$$

where $\gamma > 0$ and where U_r are the roots of

$$U_r\left[\frac{b}{\gamma} - (U_r - a)(1 - U_r)\right] = 0. \tag{4.16}$$

It is required that the system in (4.15) has a unique rest state, which can only be achieved with having a root of $U = 0$ and with having two complex roots in (4.16). In other words, in order to have a pulse solution with boundary conditions of $U(\pm\infty) = 0$, it is required that we have a homoclinic orbit about a critical point $(U, U') = (0, 0)$ in phase space. By means of this, we can obtain an equation from (4.16), given by

$$U_r - (a+1)U_r + \left(a + \frac{b}{\gamma}\right) = 0,$$

which has complex roots provided that,

$$(a+1)^2 - 4\left(a + \frac{b}{\gamma}\right) < 0. \tag{4.17}$$

Hence, upon rearranging (4.17), we obtain the following condition that needs to be satisfied, in order to obtain a pulse wave solutions:

$$(1-a)^2 < 4\frac{b}{\gamma}. \tag{4.18}$$

We shall now define an explicit finite difference scheme, to solve the FitzHugh-Nagumo equations numerically. Thus, upon substituting a forwards difference approximation for u_t and v_t, and substituting a symmetric difference approximation for u_{xx} into (4.1), then rearranging, we get

$$\begin{aligned} u_i^{j+1} &= u_i^j + r\left(u_{i+1}^j - 2u_i^j + u_{i-1}^j\right) + \Delta t\, u_i^j\left(1 - u_i^j\right)\left(u_i^j - a\right) - \Delta t\, v_i^j, \\ v_i^{j+1} &= \Delta t\,\left(bu_i^j - \gamma v_i^j\right) + v_i^j, \end{aligned} \tag{4.19}$$

where $r = \dfrac{D\Delta t}{(\Delta x)^2}$. It is required that we set a boundary condition to the left of the spacial domain. This condition is given as $u_x(0,0) = 0$. As such, we can make use of the central difference approximation to obtain $u_{-1} = u_1$ defined at this boundary.

Since we have implemented an explicit finite difference scheme, it is required that we shift the travelling wave profiles accordingly, as introduced in section 3.2.1. This is illustrated in the MATLAB code present in appendix A.2, where the explicit scheme is solved numerically.

From here, we shall investigate the affects of varying the parameters b, γ, a, and D, have on the dynamics of the system. As done previously, we shall fix parameters and vary a free parameter of the system. The following settings for the parameters will be the default values set: $\Delta x = 0.1, \Delta t = 0.005, a = 0.02, b = 0.01, \gamma = 0.02, D = 0.5$. We shall assume that these parameters remain the same for all simulations, unless stated otherwise. All simulations will run for a duration of time, $T = 500$. We shall start by investigating a change in the parameter b.

An interesting result can be observed in Figure 4.2, where the structure of the pulse waves change considerably for decreasing b.

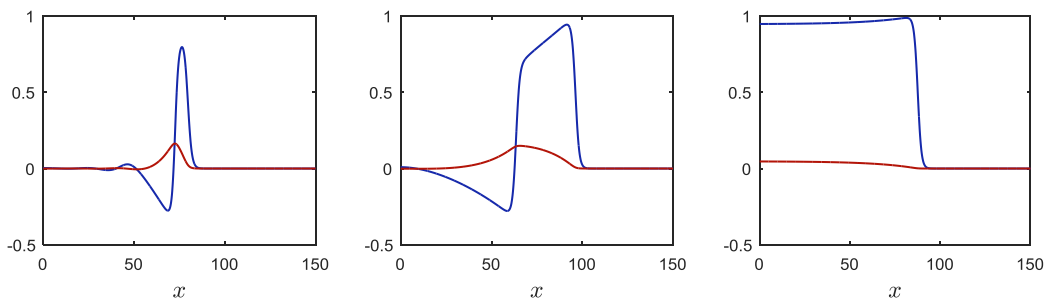

Figure 4.2: Travelling wave solutions of u (blue) and v (red), for a parameter setting of $b = 0.015$ (left), $b = 0.005$ (middle) and $b = 0.001$ (right).

The solution in u appears to deform to a shape of a wave front, where a noticeable increase in the amplitude is observed for decreasing b (Table 4.1). Furthermore, the maximum height of the wave can be seen to converge to an upper bound of approximately one. On the other hand, the solution in v diminishes and appears to approach a linear state as $b \to 0$. Also, we can observe a correlation between an increase in the

speed of the wave, with respect to decreasing b.

Table 4.1: The effects of varying the parameter b.

b	Speed c	Maximum Amplitude
0.015	0.391083913	0.795890539
0.013	0.409568478	0.839331253
0.011	0.424271174	0.870532631
0.009	0.436834478	0.896836554
0.007	0.447939087	0.920618628
0.005	0.457962435	0.942954676
0.003	0.467143261	0.964652635
0.001	0.475644174	0.986927319

An interesting phenomenon is illustrated in Figure 4.3, where the travelling pulse solutions began to collapse to a flat state, after increasing b over some threshold value. The pulse waves propagated for a duration of $T \approx 603$, where the speeds of the waves decreased as time evolved (right of Figure 4.3). In fact, this phenomenon can also be observed with the variation of the parameter a with other parameters fixed.

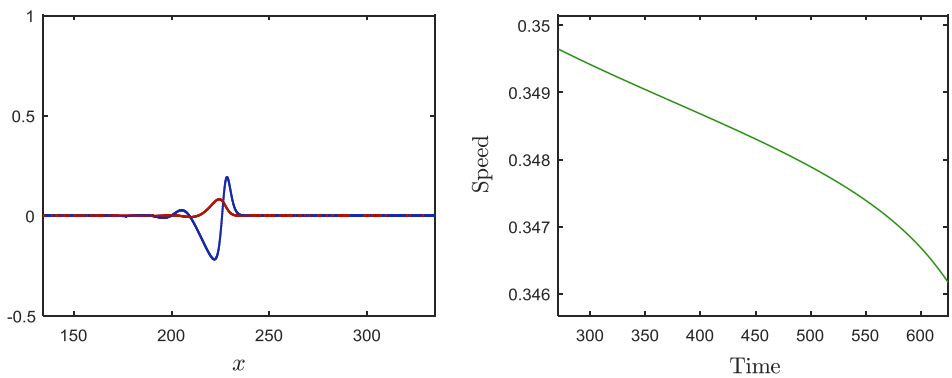

Figure 4.3: Pulse waves diminishing in size and speed after propagating for a duration of time $T \approx 625$, where $b = 0.0171$,

Consider a variation of the parameter γ with other parameters fixed (Table 4.2). We can see that the speed and the maximum height of the travelling wave solutions decreased for decreasing γ. Moreover, the travelling wave solutions in u and v deformed

in similar manners as that shown in Figure 4.2, where a correlation could be observed upon increasing g, with respect to a change in the form of the solutions.

Table 4.2: The effects of varying the parameter γ.

γ	Speed c	Maximum Amplitude
0.2	0.449356652	0.949824104
0.16	0.446655391	0.940920024
0.12	0.443383261	0.929655040
0.08	0.439312870	0.915189762
0.04	0.434054043	0.896133003
0.02	0.430767261	0.884092788
0.001	0.427054739	0.870161621

Similarly, consider a fix in the parameters, where a is varied (Table 4.3).

Table 4.3: The effects of varying the parameter a.

a	Speed c	Maximum Amplitude
0.1	0.317628391	0.813473857
0.08	0.350111043	0.843882958
0.06	0.378733174	0.861478789
0.04	0.405386261	0.874098479
0.02	0.430767261	0.884092788
0.001	0.454036957	0.892056142

We can see that the speed of the wave increases as well as the maximum height of the wave, with regards to decreasing a. Based on the analysis conducted, we can see a strong correlation between the speed of the travelling waves, with respect to the maximum height of the wave, where an increase/decrease in the height of the wave, resulted in an increase/decrease in speed.

The results produced with regards to a variation in the diffusion parameter D, were obtained with setting $\Delta x = 0.05$ and $\Delta t = 0.001$. Thus, consider a variation in the paramter D (Table 4.4).

Table 4.4: The effects of varying the parameter D.

D	Speed c	Maximum Amplitude
1	0.609558093	0.884153301
0.75	0.527889587	0.884152934
0.5	0.431014716	0.884150931
0.25	0.304762134	0.884148154
0.01	0.060844148	0.883941288

It is apparent from the table that a decrease in D resulted in the pulse wave solutions to decrease in speed dramatically. Furthermore, It can be seen from Figure 4.4, that the widths of the pulse waves decreased for decreasing D. This is intuitively expected, as reducing a parameter governing diffusion, should result in a change in width of a solution. On the other hand, we can see from Table 4.4 that the height of the waves remained the same to 4.d.p.

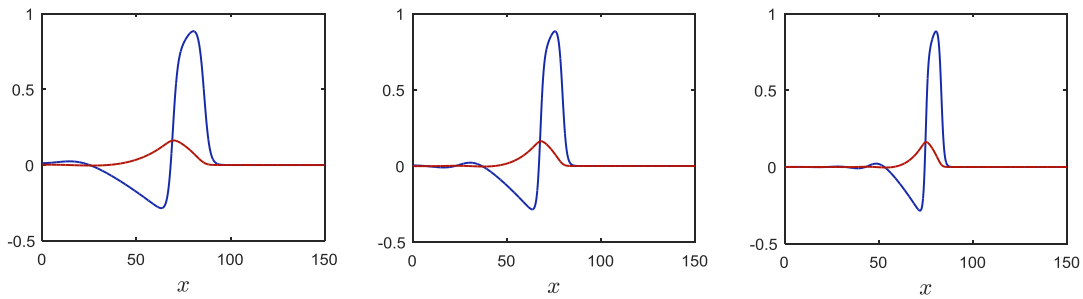

Figure 4.4: Travelling pulse solutions of u (blue) and v (red), for a parameter setting of $D = 1$ (left), $D = 0.5$ (middle) and $D = 0.25$ (right).

This concludes our analysis based on the effects of varying parameters within the system. We also observed a set of interesting results for decreasing the parameters of the system to very small values. The motivation towards conducting a finer analysis, stems from such occurrences. Thus, we shall now shift our focus to an analysis, based on the singular perturbation method, in favour of exploring the dynamics of the FitzHugh-Nagumo equations further.

4.2 Singular Perturbation Method

Within this section, we shall implement a singular perturbation method [14] to define a way in which an approximate analytical solution may be constructed for the FitzHugh-Nagumo equations. Furthermore, the method will be implemented in favour of obtaining an analytical expression for the speed c of the pulse waves, for a parameter $\epsilon \to 0$. Such a parameter will be introduced next.

We start by defining the FitzHugh-Nagumo equations with a form given by,

$$\begin{aligned} u_t &= \epsilon^2 u_{xx} + f(u) - v, \\ v_t &= \epsilon(u - v), \end{aligned} \tag{4.20}$$

where $f(u) = u(u-a)(1-u)$ with $a \in (0, \frac{1}{2})$, and where $1 \gg \epsilon > 0$. The form of the equation in (4.20) has been obtained by rescaling the variable in x. It should be noted that, the replacement of the diffusion coefficient D with ϵ^2, does not correspond to a relation between ϵ^2 and with the diffusivity of the system. Such a scaling has been introduced, to allow for a new coordinate system that will enable us to perform a finer analysis of the system. We shall now continue and rescale time by $\tau = \epsilon t$, to refine our analysis with respect to time. As of this change, we can express the equation in (4.20) as,

$$\begin{aligned} \epsilon u_\tau &= \epsilon^2 u_{xx} + f(u) - v, \\ v_\tau &= u - v. \end{aligned} \tag{4.21}$$

From here, we introduce travelling wave ansatzes for u and v, given by $u = U(z)$ and $v = V(z)$, where $z = x - c\tau$. To this end, the waves will propagate at a speed $c > 0$, towards the right of the domain. Furthermore, it is in our interest to seek a pulse wave solution of the form given in Figure 4.5. Upon substituting the ansatzes for u and v into (4.21), and then rearranging, we get,

$$\begin{aligned} \epsilon^2 U_{zz} + \epsilon c U_z + f(U) - V &= 0, \\ cV_z + U - V &= 0. \end{aligned} \tag{4.22}$$

Due to this set-up, we will assume c to be smaller or equal to $O(\epsilon^0)$. Since ϵ is very small, we can conclude that the first equation in (4.22) is in a state of equilibrium,

if $V \approx F(U)$. By means of this, it is expected that trajectories corresponding to solutions will not deviate away from this curve and will remain close.

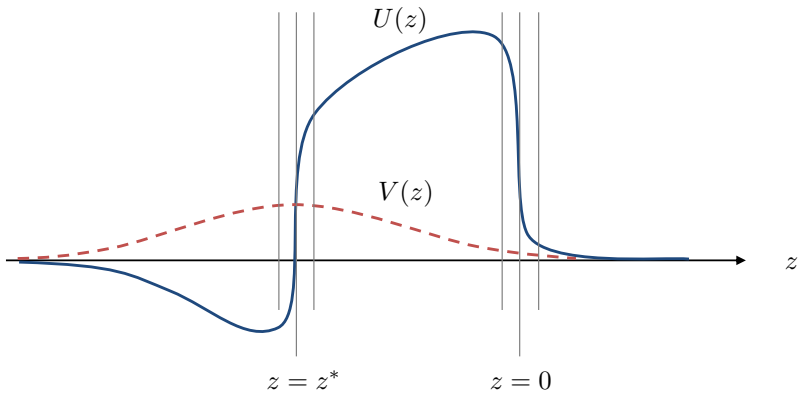

Figure 4.5: Pulse solution of the FitzHugh-Nagumo equation.

The pulse solution in Figure 4.5 has a transition layer at $z = 0$ and at $z = z^*$, where $z^* < 0$. The variable u, is known as a fast variable, and can be seen to change rapidly towards the excited regime within the transition layer at $z = 0$. The fast variable then changes rapidly to the lower branch of f, after which a steady state is achieved as $z \to -\infty$. The solution that is present in the transition layer where $z = 0$ takes a form of a wave front. Furthermore, we have a *wave back* solution in the transition layer at $z = z^*$. Since the form of a travelling wave remains fixed, the speed c of both the wave front and the wave back are the same. In order to obtain a pulse solution as seen in Figure 4.5, it is required that we determine the solution away from $z = 0$ and $z = z^*$, and then to construct the profiles that appear within the transition layers. As a consequence of this process, the speed c and the value of z^* can be determined. By means of equation (4.22), the equations defining the solution away from the transition layers are given by,

$$\begin{aligned} V &= f(U), \\ cV_z + U - V &= 0. \end{aligned} \tag{4.23}$$

This is due to the facts that ϵ is a very small quantity and that the derivatives in U are defined to being bounded. Moreover, the function $V = f(U)$ can be defined to having pseudo inverses of $P_{\pm}(V) = U$. These are shown in Figure 4.6, where the function $V = f(U)$ is set to being equivalent to $U = P_{-}(V)$ for $z > 0$ or $z < z^*$. As for $z \in (z^*, 0)$, the function $V = f(U)$ can be set to $U = P_{+}(V)$.

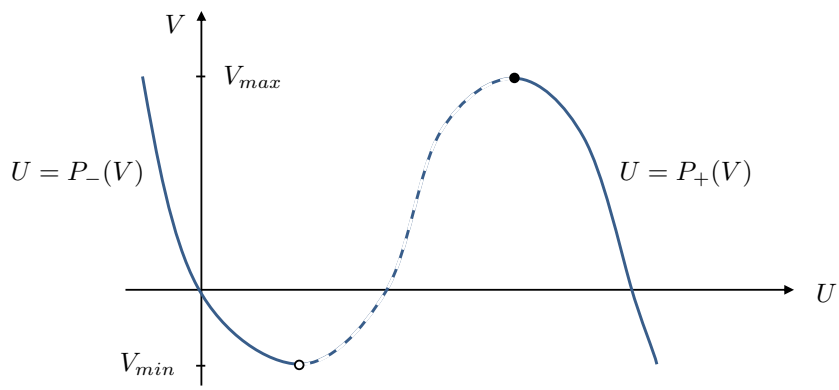

Figure 4.6: Function $V = f(U)$, where $U = P_\pm(V)$ are the pseudo inverses.

Thus, we can deduce the following sets of equations using equation (4.23). For $z > 0$, we get,

$$\begin{aligned} U &= P_-(V), \\ cV_z &= V - P_-(V), \\ \lim_{z\to\infty} V &= 0, \\ V(0) &= V_0, \end{aligned} \tag{4.24}$$

where V_0 is a constant. Similarly for $z < z^*$, we obtain

$$\begin{aligned} U &= P_-(V), \\ cV_z &= V - P_-(V), \\ \lim_{z\to-\infty} V &= 0, \\ V(z^*) &= V_1, \end{aligned} \tag{4.25}$$

where V_1 is a constant. However, for $z \in (z^*, 0)$, we get

$$\begin{aligned} U &= P_+(V), \\ cV_z &= V - P_+(V), \\ V(z^*) &= V_1, \\ V(0) &= V_0. \end{aligned} \tag{4.26}$$

In order to investigate further, the form of the differential equations present on the second line of (4.24), (4.25) and (4.26) are illustrated in Figure 4.7.

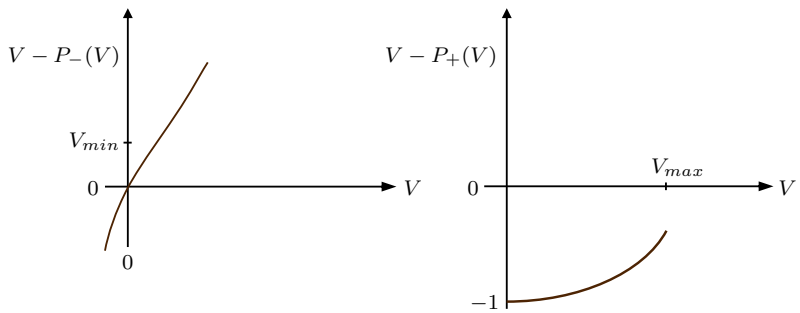

Figure 4.7: General behaviours of the cV_z term, where $cV_z = V - P_-(V)$ (left) and $cV_z = V - P_+(V)$ (right).

From (4.24), It is required that $V \to 0$ as $z \to \infty$, where we have $cV_z = V - P_-(V)$. Also, from Figure 4.7, we can see that $V - P_-(V)$ can be approximated linearly as $V \to 0$. Due to linearisation, we can obtain $cV_z = kV$, where $k > 0$. This equation can be solved to get,

$$V = V(0) \exp\left(\frac{k}{c} z\right).$$

Thus, we have an unstable equilibrium at $V = 0$, since it is required that $V \to 0$ as $z \to \infty$. To overcome this issue, we set $V(0) = 0$, yielding the constant $V_0 = 0$. As for the second equation in (4.26), by means of Figure 4.7, we have $cV_z < 0$. Hence, we can conclude that there is a smooth solution that satisfies the boundary conditions, if $0 < V_1 < V_{max}$, and where $V(z^*) = V_1$. Similarly, we can show that in (4.25), V = 0 is an unstable equilibrium in the same way as done previously. Hence, for a fixed $V_1 \in (0, V_{max})$, we can state that it is feasible to obtain a solution in the region where $z < z^*$ which satisfies the condition of $V \to 0$ as $z \to \infty$ and with $V(z^*) = V_1$. We have now established our outer solution. Thus, upon defining c and V_1, we can construct the outer profiles with regards to the transition layers, and we can obtain the values for z^*. In order to determine an expression for the speed c, we shift our focus to the transition layer at $z = 0$. Within this region, the variable V has been matched. However, the variable U must change from $U = P_-(V_0) = 0$ defined to the right of the layer, to $U = P_+(V_0) = 1$ defined to the left of the layer, for matching to occur. Such conditions become the boundary conditions within this very small region. We shall now proceed to obtaining a solution for U within this region. To do this, we start by introducing a scaling of $z = \epsilon\eta$, and with setting $U = \chi(\eta)$ and $V = \phi(\eta)$

locally at $z = 0$. Upon evaluating equation (4.22) with the state substitutions, we get

$$\begin{aligned} \chi_{\eta\eta} + c\chi_\eta + f(\chi) - \phi = 0, \\ \chi \to 0 \quad as \quad \eta \to \infty, \\ \chi \to 1 \quad as \quad \eta \to -\infty, \end{aligned} \tag{4.27}$$

$$\begin{aligned} c\phi_\eta + \eta(\chi - \phi) = 0, \\ \phi \to V_0 \quad as \quad |\eta| \to \infty. \end{aligned} \tag{4.28}$$

From here, we take the limit of $\eta \to 0$, which results in the neglection of the second term of equation (4.28). As of this occurrence, we can deduce a solution of $\phi = 0$ with the use of the boundary conditions. Hence, equation (4.27) reduces to Nagumo's equation defined in (4.2), to which we have solved previously. The speed c of the wave was obtained, and thus we can conclude that the expression governing the speed of the pulse wave in the limit of $\epsilon \to 0$, is

$$c = \frac{1}{\sqrt{2}}(1 - 2a), \tag{4.29}$$

where $c > 0$ with $a \in (0, \frac{1}{2})$. Finally, the only segment left of the pulse wave solution in Figure 4.5 to be solved for, is the section of the wave present within the transition layer at $z = z^*$. Such a solution can be obtained by a similar method to that illustrated for the transition layer at $z = 0$, but with the addition of an extra equation that needs to be solve for to determine V_1. This additional equation is obtained upon evaluating the solution at the transition layer at $z = z^*$. After combining solutions for each segment, an approximate analytical solution will be constructed.

To finalise this section, we shall numerically solve the FitzHugh-Nagumo equations present in (4.21), in favour of addressing the speed of the waves, with regards to decreasing ϵ.

We start by rearranging equation (4.21) after which we then modify to obtain an explicit finite difference scheme of the form,

$$\begin{aligned} u_i^{j+1} &= u_i^j + \epsilon r \left(u_{i+1}^j - 2u_i^j + u_{i-1}^j\right) + \frac{\Delta t}{\epsilon}\left[u_i^j\left(1 - u_i^j\right)\left(u_i^j - a\right) - v_i^j\right], \\ v_i^{j+1} &= \Delta t \left(u_i^j - v_i^j\right) + v_i^j, \end{aligned} \tag{4.30}$$

where $r = \dfrac{D\Delta t}{(\Delta x)^2}$. We retain the same boundary condition as stated previously within this chapter, namely $u_x(0,0) = 0$, resulting in $u_{-1} = u_1$. The code to simulate this finite difference scheme can be found in appendix A.3.

To produce the results depicted in Table 4.5, the following parameters were set: $\Delta x = 0.02, dt = 0.000012, T = 20, a = 0.03$.

Table 4.5: Numerical approximations of the speed of the pulse wave, with regards to decreasing ϵ, where an exact solution of $c = 0.664680374$ has been obtained.

ϵ	Speed c
0.012	0.567236467
0.010	0.588623932
0.008	0.606905983
0.006	0.623014245
0.004	0.637225071
0.002	0.647951567

It is evident in Table 4.5 that the speed of the pulse waves converged towards the exact solution of $c = 0.664680374$ for decreasing ϵ. Furthermore, it was observed that the width of the wave decreased for decreasing ϵ. It is expected that upon decreasing ϵ further, the numerical approximations of the speed will converge to the exact solution.

In summary, the parameters associated with the FitzHugh-Nagumo equations were shown to affect the dynamics of the system extensively. We observed a deformation in the pulse solution in u, to which it changed forms to resemble a wave front for a variation in the parameters b and g. Based on the analysis conducted, it was possible to identify a strong relation between the speed of the wave, and with regards to its maximum height. We then conducted a singular perturbation method, where the method behind the construction of approximate analytical solutions for the FitzHugh-Nagumo equations were covered. From this, we obtained an exact solution that defined the speed of the travelling waves in the limit of $\epsilon \to 0$. Finally, we performed a numerical validation of the proposed solution, to a certain degree of accuracy.

Chapter 5

Conclusions

In the beginning stages of this project, we investigated the Burgers-Huxley equation in favour of determining its dynamics with respect to the parameters k, m and n. This was done at an initial stage by solving the equation numerically with the use of an explicit finite difference scheme. It was shown that the speed of the wave diminished the most for increasing m, as compared to increasing n or k. Furthermore, the travelling wave solutions converged to a unique state, which lead to the questioning of the existence of solutions. After this, the Burgers-Huxley equation was solved for special solutions, with the use of the factorisation method. From here, the concept of the existence of solutions was further explored with the use of phase plane analysis. As such, it was shown that an infinite number of feasible travelling wave solutions exist, for the two cases, namely $m = 1$ and $m > 1$. Such solutions were determined with the use of power series approximations that were constructed to model a heteroclinic orbit in phase space. The project then leads onto the investigation of the FitzHugh-Nagumo equations, where the dynamics were also explored with respect to the parameters a, γ, D and b. This was done via the use of an explicit scheme, where the parameters associated with the equations were subject to an imposing condition, for a feasible pulse solution to be generated. We observed a deformation in the pulse wave solution in u, after which it changed forms to resemble a wave front solution for a variation in b. From the analysis conducted, a strong relation that related the speed of the wave, with its amplitude was stated. Such a relation was observed for all parameters involved within the equations. After this section, a singular perturbation method was

conducted, where an approximate analytical solution was covered. As of this analysis, an expression representing the travelling pulse speed was derived. The expression in c was then numerically validated. This concludes the highlights of our findings within this thesis. In the next section, the concept of further research will be covered.

5.0.1 Further research

Within this section, we shall state the future areas of research in bullet point form. Thus, for the Burgers-Huxley equation:

- To investigate why we have one travelling wave solution corresponding to exponential decay for $m > 1$.
- To include non-linear terms that were omitted when performing a phase plane analysis, in favour of investigating the dynamics further.
- To explore different methods for solving the Burgers-Huxley equation in favour of obtaining a different set of special solutions.
- To employ different methods to determine the dynamics of the Burgers-Huxley equation, with regards to varying k, m and n.
- To investigate the equation with a different set of parameter variations.

For the FitzHugh-Nagumo equations:

- To explore the dynamics of the system further, with respect to the parameters of the system.
- To derive an approximate analytical solution, based on the underlying theory of the singular perturbation method.
- To conduct a three dimensional phase plane analysis, in favour of exploring the dynamics of the FitzHugh-Nagumo equations further.

Appendix A

Programming Codes

A.1 Numerical Simulation of the Burgers-Huxley Equation

```
% This program implements an explicit scheme to solve the Burgers-Huxley
% eqution, with the addition of shifting the profile. The code ...
    outputs the
% travelling wave profile, with its corresponding speeds with respect to
% variation in time.
clear all; clc;
% Spacial increment.
dx = 0.1;
% Time increment.
dt = (0.95)*(1/2)*dx^2;
% Initial spacial domain.
x = [-20:dx:20];
% Time frame for simulation.
T = 600;
% Initial conditions.
u = (1-tanh(x))/2;
% Parameters k,m and n.
pk = 1; pm = 1; pn = 1;

```

```
% Defining initail states of paramters that will be used in the program.
iter = 1;
cumshift = 0;
xoffset = 0;
xpos = 0;
tm = 0;
% Implementing a shift every 300th iteration.
for j = 0:dt:T
% Applying a numerical shift every .
if (mod(iter,300)==0)
figure(1)
% Returns indices of the vector "u" that agree with the condition.
ind = find(u>0.1 & u<0.9);
% Returns the x value that corresponds to the u value at 0.5.
xc = interp1(u(ind),x(ind),0.5);
% Determining the number of steps xc is away from 0.
N = floor(xc/dx);
% Creating shift variable.
xshift = N*dx;
% Cumulated shift.
cumshift = cumshift + xshift;
% Rounding error.
xoffset = xc - xshift;
% Creating shifted u.
u = [u(N+1:end) zeros(1,N)];
% Shifting x domain.
newx = x+cumshift;
% Plotting shifting wave solution.
plot(newx,u,'b');
axis([newx(1) newx(end) -0.1 1.1])
pause(0.01)
% Adding the total shift to a vector.
xpos = [xpos cumshift+xoffset];
% Adding the accumulated time frames between shits.
tm = [tm j];
end
% Explicit scheme.
u(2:end-1) = u(2:end-1) + ...
    (dt/(dx)^2).*(u(3:end)-2.*u(2:end-1)+u(1:end-2)) ...
```

```
- (dt/(2*dx)).*u(2:end-1).^pk.*(u(3:end) - u(1:end-2)) ...
+ dt.*u(2:end-1).^pm.*(1-u(2:end-1).^pn);
% Boundary conditions.
u(1) = 1;
u(length(x)) = 0;
iter = iter+1;
end
% Defining parameter values.
sum = 0;
k = 0;
speed(1) = 0;
% Computing the speeds with respect to time.
for j = 2:length(xpos)
g = (xpos(j)-xpos(j-1))/(tm(j)-tm(j-1));
sum = sum + g;
k = k+1;
speed(j) = sum/k;
end
figure (4)
% Plotting a Speed vs Time graph.
plot(tm,speed)
fprintf('final speed = %1.9f\n', speed(end));
```

A.2 Numerical Simulation of the FitzHugh-Nagumo Equation

```
% This code implements an explicit scheme to solve the FitzHugh-Nagumo
% equation, where a shifting is implemented.
clear all; clc;
% Spacial increment.
dx = 0.1;
% Time increment.
dt = (1/2)*dx^2;
% Initial spacial domain.
```

```
x = [0:dx:200];
% Time frame for simulation.
T = 500;
% Initial conditions.
d = 1;
u = 1.1*exp(-x.^2/d^2);
v = zeros(1,length(x));
% Parameters.
D = 0.5;
r = D*dt/dx^2;
a = 0.02;
b = 0.01;
g = 0.02;

% Defining intial values for parameters used within the program.
iter = 0;
cumshift = 0;
xoffset = 0;
xpos = 0;
tm = 0;
% Defining a vector in x that will be used within the shifting process.
newx = x;
% Implementing the time marching scheme.
for j = 0:dt:T
% Explicit scheme.
v = dt.*(b*u - g*v) + v;
u(2:end-1) = u(2:end-1) + r.*(u(3:end)-2.*u(2:end-1)+u(1:end-2)) ...
+ dt.*u(2:end-1).*(1-u(2:end-1)).*(u(2:end-1)- a) -  dt.*v(2:end-1);
% Boundary conditions
u(1) = u(1) + 2*r*(u(2) - u(1)) + dt*(u(1)*(1-u(1))*(u(1)-a)) - dt*v(1);
u(end) = 0;

% Variable used to start the shifting process
tstart = 267;
if(j ≥ tstart)
iter = iter + 1;
% Defining starting point to which the shift will be implement.
if (tj == 0)
xq = [x(1):0.001:x(end)];
```

```
s = interp1(x,u,xq,'spline');
maxs = max(s);
mxu = find(s==max(s));
xcm = xq(mxu);
tj = j;
end
% Plotting solutions of the travelling wave with regards to the
% implementation of a shift.
if (mod(iter,400)==0)
w = find(u>0.2);
ww = x(w);
xq2 = [ww(1):0.00001:ww(end)];
% Using the interp1 function to obtain the maximum height of
% the wave in solution u.
h = interp1(x,u,xq2,'spline');
ind = find(h == max(h));
% Implementing the shifting technique
xt = xq2(ind);
xc = xt - xcm;
N = floor(xc/dx);
% Generating the required shift.
xshift = N*dx;
cumshift = cumshift + xshift;
xoffset = xc - xshift;
% Shifting u and v.
u = [u(N+1:end) zeros(1,N)];
v = [v(N+1:end) zeros(1,N)];
% Plotting shifting solutions.
plot(newx,u,'r',newx,v,'g');
axis([newx(1) newx(end) -0.5 1])
xlabel('$x$','Interpreter','latex','Fontsize',13);
ylabel('$u$','Interpreter','latex','Fontsize',13);
newx = x+cumshift+ xoffset;
pause(0.01)
xpos = [xpos cumshift+xoffset];
tm = [tm j];
end
end
end
```

```
% Calculating the speed of the waves.
sum = 0;
k = 0;
speed(1) = 0;
% Calculating the speed of the traveling wave with respect to time.
for j = 3:length(xpos)
temp = (xpos(j)-xpos(j-1))/(tm(j)-tm(j-1));
sum = sum + temp;
k = k+1;
speed(j) = sum/k;
end
% Plotting the speed vs time.
figure (4)
plot(tm(3:end),speed(3:end))
axis([tm(3) tm(end) (speed(end)-0.0005) (max(speed)+0.0005)])
xlabel('Time','Interpreter','latex','Fontsize',11);
ylabel('Speed','Interpreter','latex','Fontsize',11);
fprintf('final speed = %1.9f\n', speed(end));
fprintf('maximum of u = %1.9f\n', max(u));
```

A.3 Numerical Simulation of the FitzHugh-Nagumo Equation with ϵ

```
% This code implements an explicit scheme to solve the FitzHugh-Nagumo
% equation with epsilon, where a shifting is implemented.
clear all; clc;
% Spacial increment.
dx = 0.02;
% Time increment.
dt = (3)*dx^2;
% Initial spacial domain.
x = [0:dx:5];
% Time frame for simulation.
T = 20;
```

```
% Initial conditions.
d = 1;
u = 1.1*exp(-x.^2/d^2);
v = zeros(1,length(x));
% Parameters.
eps = 0.012;
r = dt/dx^2;
a = 0.03;

% Defining intial values for parameters used within the program.
iter = 0;
cumshift = 0;
xoffset = 0;
xpos = 0;
tm = 0;
tj = 0;
kk = 0;
% Defining a vector in x that will be used within the shifting process.
newx = x;
% Implementing the time marching scheme.
for j = 0:dt:T
% Explicit scheme.
v = dt.*(u - v) + v;
u(2:end-1) = u(2:end-1) + eps*r.*(u(3:end)-2.*u(2:end-1)+u(1:end-2)) ...
+ (dt/eps).*u(2:end-1).*(1-u(2:end-1)).*(u(2:end-1)- a) -  ...
    (dt/eps).*v(2:end-1);
% Boundary conditions
u(1) = u(1) + 2*eps*r*(u(2) - u(1)) + ...
    (dt/eps)*(u(1)*(1-u(1))*(u(1)-a)) - (dt/eps)*v(1);
u(end) = 0;

% Variable used to start the shifting process
tstart = 2.5;
if(j ≥ tstart)
iter = iter + 1;
% Defining starting point to which the shift will be implement.
if (tj == 0)
xq = [x(1):0.001:x(end)];
s = interp1(x,u,xq,'spline');
```

```
maxs = max(s);
mxu = find(s==max(s));
xcm = xq(mxu);
tj = j;
end
% Plotting solutions of the travelling wave with regards to the
% implementation of a shift.
if (mod(iter,400)==0)
w = find(u>0.2);
ww = x(w);
xq2 = [ww(1):0.00001:ww(end)];
% Using the interp1 function to obtain the maximum height of
% the wave in solution u.
h = interp1(x,u,xq2,'spline');
ind = find(h == max(h));
% Implementing the shifting technique
xt = xq2(ind);
xc = xt - xcm;
N = floor(xc/dx);
% Generating the required shift.
xshift = N*dx;
cumshift = cumshift + xshift;
xoffset = xc - xshift;
% Shifting u and v.
u = [u(N+1:end) zeros(1,N)];
v = [v(N+1:end) zeros(1,N)];
% Plotting shifting solutions.
plot(newx,u,'r',newx,v,'g');
axis([newx(1) newx(end) -0.5 1])
xlabel('$x$','Interpreter','latex','Fontsize',13);
ylabel('$u$','Interpreter','latex','Fontsize',13);
newx = x+cumshift+ xoffset;
pause(0.01)
xpos = [xpos cumshift+xoffset];
tm = [tm j];
end
end
end
% Calculating the speed of the waves.
```

```
sum = 0;
k = 0;
speed(1) = 0;
% Calculating the speed of the traveling wave with respect to time.
for j = 3:length(xpos)
temp = (xpos(j)-xpos(j-1))/(tm(j)-tm(j-1));
sum = sum + temp;
k = k+1;
speed(j) = sum/k;
end
% Plotting the speed vs time.
figure (4)
plot(tm(length(tm)/3:end),speed(length(speed)/3:end));
axis([tm(3) tm(end) 0 (speed(end)+0.2)])
fprintf('final speed = %1.9f\n', speed(end));
```

A.4 Power Series Approximations for all m

```
> restart:
```

Loading the required packages.

```
> with(powseries):
> with(plots):
```

Defining the number of terms in the power series.

```
> s := 9:
```

Parameters k, m and n.

```
> k := 1:  m := 1:  n := 1:
```

Defining the power series of $w(v) = a_s \cdot v^s$.

```
> powcreate(w(s) = a[s]);
```

The command *tpsform* has been added to illustrate the power series up to order 10.

```
> tpsform(w,v,10);
```

Defining all the terms present in the equation $v\dfrac{dw}{dv} + c\,(w) - v^k\,(w) + v^m\,(1 - v^n)$, as power series.

```
> wsd := powdiff(w):
> c1 := powpoly(c,v):
> c2 := powpoly(-v^k,v):
> c3 := powpoly(v^m*(1-v^n),v):
> ws := powint(wsd):
```

Defining a temporary equation of $w\,(v)$, which will be used to plot the power series solutions.

```
> equ3 := convert(tpsform(ws, v, s+1), polynom):
```

Using the commands powadd/multiply to formulate the equation.

```
> equ := powadd(multiply(ws,wsd),multiply(c1,ws),multiply(c2,ws),c3);
```

Factoring out terms in v , after generating the equation defined as a power series.

```
> equ := tpsform(equ,v,s+1);
```

Truncating the power series.

```
> equ := convert(equ,polynom);
```

Generating a list of the coefficients in v equated to zero.

```
> con := {seq(coeff(equ,v,i)= 0,i = 1..s)};
```

Solving the system of equations, to obtain solutions for the coefficients a_s in terms of the speed c.

```
> sol := solve(con,{seq(a[i], i = 1..s)}):
```

Assigning the solutions in a_s from the list *sol*, to the workspace.

```
> assign(sol);
```

Generating the equation $a_1 + a_2 + ... + a_s = 0$, obtained with the use of the boundary condition $w\,(1) = 0$.

```
> equ2 := add(a[i],i = 1..s) = 0:
```

Solving the equation defined in *equ2*, to obtain solutions for $c > 0$.

```
> cval := select(type,[evalf(solve(equ2,c))],'positive');
```

Specifying the number of incorrect power series solutions with respect to c for a polynomial of 9 terms, to aid in plotting solutions. The infeasible solutions in c can be observed to be the last 6 terms of the vector *cval*.

```
> er := 6:
```

Plotting the heteroclinic orbits for a range of c values, acknowledging the fact that the *cval* vector contains c values that are ordered in a descending order.

```
> for j from 1 to (nops(cval)-er) do
> c := cval[j];
> col := ColorTools:-Color([0.15*j,0,0]):
> p||j := plot(equ3,v = 0..1, color = col, axesfont = [Latex, 10],
> labelfont = ["Latex", 15], labels = ['v','w']);
> od:
> display({seq(p||j,j = 1 ..  (nops(cval)-er))});
```

A.5 Power Series Approximations with setting $m > 1$ and $a_1 = 0$

```
> restart:
```

Loading the required packages.

```
> with(powseries):
> with(plots):
```

Defining the number of terms in the power series.

```
> s := 30:
```

Parameters k, m and n.

```
> k := 1:  m := 2:  n := 1:
```

Defining the power series of $w(v) = a_s \cdot v^s$.

```
> powcreate(w(s) = a[s]);
```

Setting $a_0 = a_1 = 0$.

```
> a[0] := 0:  a[1] := 0:
```

The command *tpsform* has been added to illustrate the power series up to order 10.

```
> tpsform(w,v,10);
```

Defining all the terms present in the equation $v\dfrac{dw}{dv} + c(w) - v^k(w) + v^m(1 - v^n)$, as power series.

```
> wsd := powdiff(w):
> c1 := powpoly(c,v):
> c2 := powpoly(-v^k,v):
> c3 := powpoly(v^m*(1-v^n),v):
> ws := powint(wsd):
```

Defining a temporary equation of $w(v)$, which will be used to plot the power series solutions.

```
> equ3 := convert(tpsform(ws, v, s+1), polynom):
```

Using the commands powadd/multiply to formulate the equation.

```
> equ := powadd(multiply(ws,wsd),multiply(c1,ws),multiply(c2,ws),c3);
```

Factoring out terms in v, after generating the equation defined as a power series.

```
> equ := tpsform(equ,v,s+1);
```

Truncating the power series.

```
> equ := convert(equ,polynom);
```

Generating a list of the coefficients in v equated to zero.

```
> con := {seq(coeff(equ,v,i)= 0,i = 2..s)};
```

Solving the system of equations, to obtain solutions for the coefficients a_s in terms of the speed c.

```
> sol := solve(con,{seq(a[i], i = 2..s)}):
```

Assigning the solutions in a_s from the list *sol*, to the workspace.

```
> assign(sol);
```

Generating the equation $a_2 + a_3 + ... + a_s = 0$, obtained with the use of the boundary condition $w(1) = 0$.

```
> equ2 := add(a[i],i = 2..s) = 0:
```

Solving the equation defined in *equ2*, to obtain solutions for $c > 0$.

```
> cval := select(type,[evalf(solve(equ2,c))],'positive');
```

Specifying the number of incorrect power series solutions with respect to c for a polynomial of 30 terms, to aid in plotting solutions. The infeasible solutions in c can be observed to be the first 8 terms of the vector *cval*.

```
> er := 8:
```

Plotting the heteroclinic orbits for a range of c values, acknowledging the fact that the *cval* vector contains c values that are ordered in a ascending order.

```
> for j from er to (nops(cval)) do
> c := cval[j];
> col := ColorTools:-Color([0.15*(nops(cval)+1-j),0,0]):
> p||j := plot(equ3,v = 0..1, color = col, axesfont = [Latex, 10],
> labelfont = ["Latex", 15], labels = ['v','w']);
> od:
> display({seq(p||j,j = er ..  (nops(cval)))});
```

Bibliography

[1] ODE Software for MATLAB. http://www.math.rice.edu/~dfield/, 2016. [Online; accessed 01-August-2016].

[2] The depolarised neuron (a stimulated neuron). http://tle.westone.wa.gov.au/content/file/969144ed-0d3b-fa04-2e88-8b23de2a630c/1/human_bio_science_3b.zip/content/002_nervous_control/page_11.htm, 2016. [Online; accessed 09-May-2016].

[3] M. Ablowitz and B. Fuchssteiner. *Topics in Soliton Theory and Exactly Solvable Nonlinear Equations*. World Scientific Pub Co Inc, 1987.

[4] K. Al-Khaled. Sinc numerical solution for solitons and solitary waves. *Journal of Computational and Applied Mathematics*, 130(12):283 – 292, 2001.

[5] L. M. Berkovich. Factorization as a method for finding exact invariant solutions of the Kolmogorov-Petrovskiĭ-Piskunov equation and related equations of Semenov and Zeldovich. dovich. *Dokl. Akad. Nauk*, pages 823–827, 1992.

[6] F. Browder et al. Partial differential equations in the 20th century. *Advances in Mathematics*, 135(1):76–144, 1998.

[7] D. Brown, J. Feng, and S. Feerick. Variability of firing of hodgkin-huxley and fitzhugh-nagumo neurons with stochastic synaptic input. *Physical Review Letters*, 82(23):4731, 1999.

[8] A. Champneys, G. Hunt, and J. Thompson. *Localization and Solitary Waves in Solid Mechanics*. Advanced series in nonlinear dynamics. World Scientific, 1999.

[9] O. Cornejo-Prez and H. C. Rosu. Nonlinear second order ode's: Factorizations and particular solutions. *Progress of Theoretical Physics*, 114(3):533–538, 2005.

[10] M. El-Azab. An approximation scheme for a nonlinear diffusion fishers equation. *Applied Mathematics and Computation*, 186(1):579 – 588, 2007.

[11] S. A. El-Wakil and M. A. Abdou. New exact travelling wave solutions using modified extended tanh-function method. *Chaos Solitons Fractals*, 31(4):840–852, 2007.

[12] L. Evans. *Partial Differential Equations*. Graduate studies in mathematics. American Mathematical Society, 1998.

[13] E. Fan. Extended tanh-function method and its applications to nonlinear equations. *Physics Letters A*, 277(45):212 – 218, 2000.

[14] P. Grindrod. *The Theory and Applications of Reaction-diffusion Equations: Patterns and Waves*. Oxford applied mathematics and computing science series. Clarendon Press, 1996.

[15] G. Hariharan, K. Kannan, and K. Sharma. Haar wavelet method for solving fishers equation. *Applied Mathematics and Computation*, 211(2):284 – 292, 2009.

[16] J.-H. He and X.-H. Wu. Exp-function method for nonlinear wave equations. *Chaos Solitons Fractals*, 30(3):700–708, 2006.

[17] W. Hereman and A. Nuseir. Symbolic methods to construct exact solutions of nonlinear partial differential equations. *Mathematics and Computers in Simulation*, 43(1):13 – 27, 1997.

[18] H. Jafari, A. Sooraki, Y. Talebi, and A. Biswas. The first integral method and traveling wave solutions to davey-stewartson equation. *Nonlinear Anal.-Model. Control*, 17:182–193, 2012.

[19] N. A. Kudryashov. Partial differential equations with solutions having movable first-order singularities. *Physics Letters A*, 169(4):237 – 242, 1992.

[20] W. Likus and V. Vladimirov. Solitary waves in the model of active media, taking

into account effects of relaxation. *Reports on Mathematical Physics*, 75(2):213 – 230, 2015.

[21] J. Murray. *Mathematical Biology.* Biomathematics. Springer Berlin Heidelberg, 2013.

[22] J. A. Pojman, V. M. Ilyashenko, and A. M. Khan. Free-radical frontal polymerization: self-propagating thermal reaction waves. *J. Chem. Soc., Faraday Trans.*, 92(16):2825–2837, 1996.

[23] M. M. Rashidi, D. D. Ganji, and S. Dinarvand. Approximate traveling wave solutions of coupled Whitham-Broer-Kaup shallow water equations by homotopy analysis method. *Differ. Equ. Nonlinear Mech.*, pages Art. ID 243459, 8, 2008.

[24] J. Smoller. *Shock waves and reactiondiffusion equations*, volume 258. Springer Science & Business Media, 2012.

[25] H. C. Tuckwell and R. Rodriguez. Analytical and simulation results for stochastic fitzhugh-nagumo neurons and neural networks. *Journal of Computational Neuroscience*, 5(1):91–113, 1998.

[26] A. Volpert. *Traveling wave solutions of parabolic systems.*

[27] X. yi Wang. Nerve propagation and wall in liquid crystals. *Physics Letters A*, 112(8):402 – 406, 1985.

[28] Y. Zhang, WenshengDai. Finite-difference solution of the helmholtz equation based on two domain decomposition algorithms. *Journal of Applied Mathematics and Physics*, 01(04):18–24, 2013.

[29] Z. Zhang and J. Wang. On the similarity solutions of magnetohydrodynamic flows of power-law fluids over a stretching sheet. *Journal of Mathematical Analysis and Applications*, 330(1):207 – 220, 2007.